The Emergence of Compartmental Organization in the Olfactory Bulb Glomerulus

Hanna Klein

YALE UNIVERSITY

2000

The Emergence of Compartmental Organization in the Olfactory Bulb Glomerulus

A Thesis Submitted to the
Yale University School of Medicine
In Partial Fulfillment of the Requirements for the
Degree of Doctor of Medicine

by
Hanna Kim
2000

Abstract

The olfactory bulb glomerulus is a discrete and heterogeneous neuropil where olfactory receptor cell axons synapse with dendrites of mitral, tufted and periglomerular neurons. In the first study, we investigated the organization of the glomerular neuropil by using antibodies to both single and double-labeled constituents for analyses with confocal microscopy. Electron microscopy was used to assess the distribution of synapses within the glomerulus. The olfactory bulbs of adult Sprague-Dawley rats were processed for immunocytochemistry with olfactory marker protein (OMP), synaptophysin, synapsin 1, glial fibrillary acidic protein (GFAP) and/or microtubule associated protein 2 (MAP2). Double labeling for OMP and MAP2 revealed two distinct subcompartments within glomeruli. Synaptophysin and synapsin 1 also showed differential labeling with the glomerulus. Electron micrograph reconstructions of glomeruli revealed interdigitating axonal and dendritic subcompartments, where primary afferent axodendritic and local circuit dendrodendritic synapses segregated within the glomerulus into the axonal and dendritic subcompartments, respectively. These results support the hypothesis of subcompartmental organization within olfactory bulb glomeruli. In the second study, we employed similar techniques to better understand the maturation of glomeruli and to examine the spatio-temporal interactions that occur during postnatal development. Sprague-Dawley rats at postnatal days 1, 6, 12, and 18 were processed for single and double label immunocytochemistry for OMP, growth associated protein (GAP-43), and synaptophysin. Mature adult-like subcompartmental organization within the glomerulus emerged by postnatal day 12. Earlier in development immature axons entered the core of the glomerulus and moved to the periphery as they matured. However, beginning around 12 days postnatal, immature axons distributed in the periphery and moved toward the core as they matured. This change in the trajectories of axons into glomeruli suggests that different rules may be followed in establishing versus maintaining glomeruli.

Acknowledgements

I would first like to thank Dr. Charles A. Greer for his unfailing and unconditional support. Since we first met seven years ago, Dr. Greer has not only been my advisor, but also my greatest mentor and steady friend. He has guided and inspired me throughout my pursuit of science, knowledge, and my career in medicine, and to him I will always be indebted. I would also like to thank my colleagues and friends in the lab, including Hahnah Kasowski, Helen Treloar, Brian Lipscomb, Kara Salvagno, Chris Kaliszewski, Karl Kafitz, and Kenny Chiu for all their kindness and help, especially if it concerned any chocolate lying around the lab.

I would like to thank my friends and family, who have given me all the strength, love, and support I could hope for. I am truly blessed. Thanks Mom, Dad, Anna, Andrew, and Grandma!

Table of Contents

Page

Introduction....1

The Olfactory System: An Overview....1

Glomerulus as a Functional Unit....4

Heterogeneity of the Glomerulus....8

Development of the Glomerulus....9

Statement of purpose and hypothesis....10

Materials and Methods....12

Adults....12

Developmental....17

Results....22

Adults....22

Developmental....44

Discussion....76

References....92

Figures....100

Figure 1: An overview of the anatomy of the olfactory system. Olfactory receptor cells located in the olfactory epithelium project to the olfactory bulb to make synapses with mitral and tufted cells. These neurons form the output of the olfactory bulb and project to the olfactory cortex. The olfactory bulb exhibits a distinctly laminar organization, each layer containing highly differentiated cell types. It has recently been demonstrated that the olfactory epithelium may be divided into four distinct spatial zones (roman numerals I-IV). In each of these zones a distinct and nonoverlapping set of olfactory receptors are expressed. Abbreviations: AOB, accessory olfactory bulb; c.f., centrifugal fiber; G_d, deep granule cell; G_s, superficial granule cell; M, mitral cell; OSN, olfactory receptor cell; P, periglomerular cell; r.c., recurrent collateral; T, tufted cell. (From Shepherd and Greer, 1997)

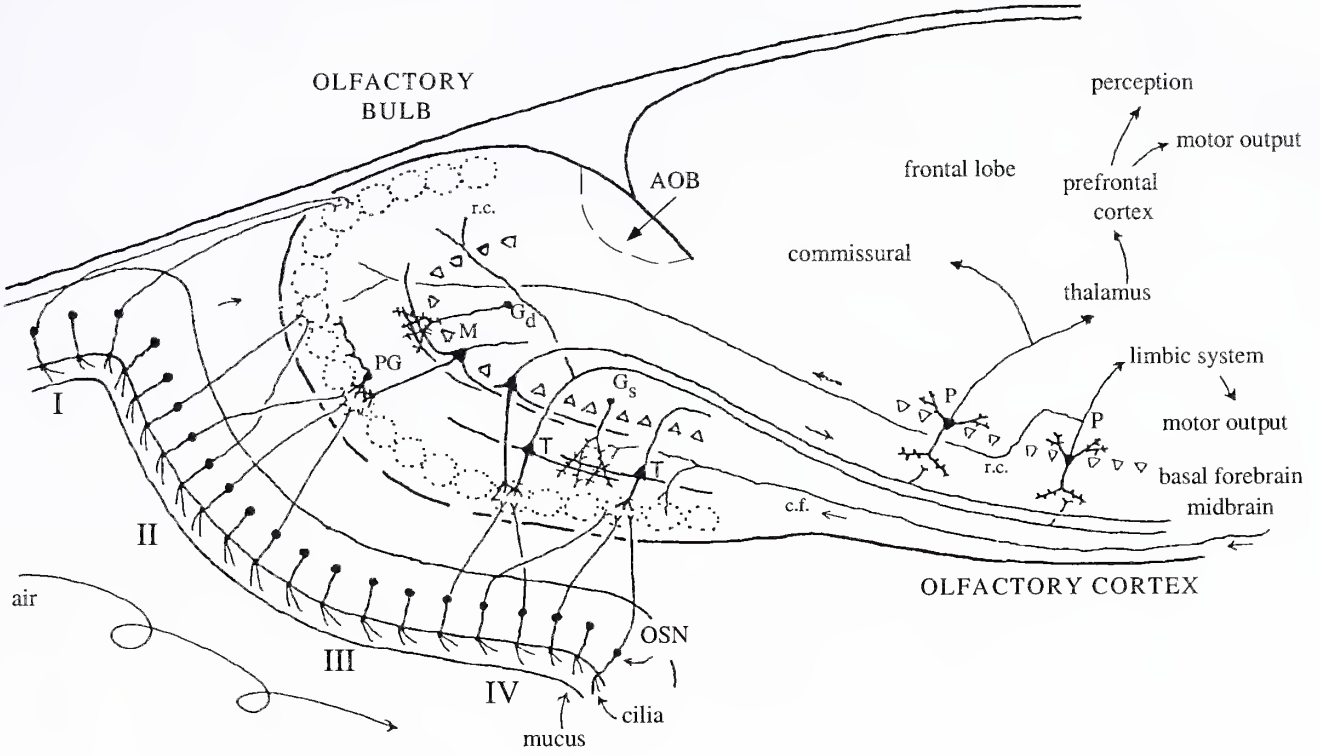
OLFACTORY
BULB
AOB
r.c.
M
G_d
PG
G_s
T
T
I
II
III
IV
air
OSN
cilia
mucus
perception
motor output
frontal lobe
prefrontal
cortex
commissural
thalamus
limbic system
motor output
P
P
r.c.
basal forebrain
midbrain
c.f.
OLFACTORY CORTEX

The Glomerulus as a Functional Unit

The glomerulus is a complex and discrete neuropil that is the site of the initial synapse in the olfactory pathway. Each olfactory receptor cell terminates in a single glomerulus, while the primary dendrite of each mitral and tufted cell also enters a single glomerulus. Studies in the rabbit have estimated that a single glomerulus receives input from 25,000 olfactory receptor cell axons, and that about 25 mitral cells and 10-15 tufted cells send dendritic processes to each glomerulus (Allison and Warwick, 1949). These spherical structures range from 30-100 μm in diameter (Allison and Warwick, 1949; Baier and Korsching, 1994) and number between 1000-3000 depending on the species, approximately 3000 in rats (Meisami and Safari, 1981).

There is increasing evidence that the olfactory bulb glomerulus serves as a fundamental organizational unit in odor coding. Functional analyses of the rat olfactory bulb using activity mapping studies with 2-deoxyglucose have demonstrated that specific odorants produced spatially defined patterns of glomerular activity in the olfactory bulb (Stewart et al., 1979; Greer et al., 1982). Moreover, these patterns of 2-deoxyglucose uptake elicited by different odors appear distinct for different odors. Similar results have been obtained using c-FOS immunocytochemistry (Guthrie et al., 1995). In addition, optical recordings of the olfactory bulb using voltage sensitive dyes have also demonstrated that single odors produce diffuse yet circumscribed patterns of activity (Kauer et al., 1987).

Electrophysiologic studies have further shown that mitral cells associated with individual glomeruli respond differentially or are "tuned" to specific odorants (Buonviso

and Chaput, 1990; Mori et al., 1992). Indeed, extracellular spike responses recorded from single mitral cells were found to be maximally responsive to a specific odorant.

Figure 2: Basic synaptic circuitry of the olfactory bulb. Olfactory receptor cell axons form synapses with the dendrites of mitral, tufted, and periglomerular neurons. Periglomerular cells are interneurons, forming interglomerular connections. Mitral and tufted cells are the output neurons and project to the olfactory bulb. Further odor processing occurs via granule cells, which form synapses with mitral and tufted cells. ONL, olfactory nerve layer; GLOM, glomerular layer; EPL, external plexiform layer; MCL, mitral cell layer; GL, granule cell layer; ON, olfactory nerve fiber; PG, periglomerular cell; Tm, tufted cell; M1, mitral cell; Gd, deep granule cell; Gs, superficial granule cell; LOT, lateral olfactory tract. (From Shepherd, 1990)These studies are consistent with the recent demonstration that axons terminating in any one glomerulus are derived from olfactory receptor neurons that express the same putative odor receptor (Ressler et al., 1994; Vassar et al., 1994; Mombaerts et al., 1996). Thus each glomerulus in the mammalian olfactory bulb expresses a specific molecular phenotype based on the subpopulation of receptor cells that innervate the glomerulus. These studies provide strong support for the notion that the topographic projections of olfactory receptor cell axons onto glomeruli provide the basis for a highly organized and spatially stereotyped map that encodes odor quality in the olfactory bulb.

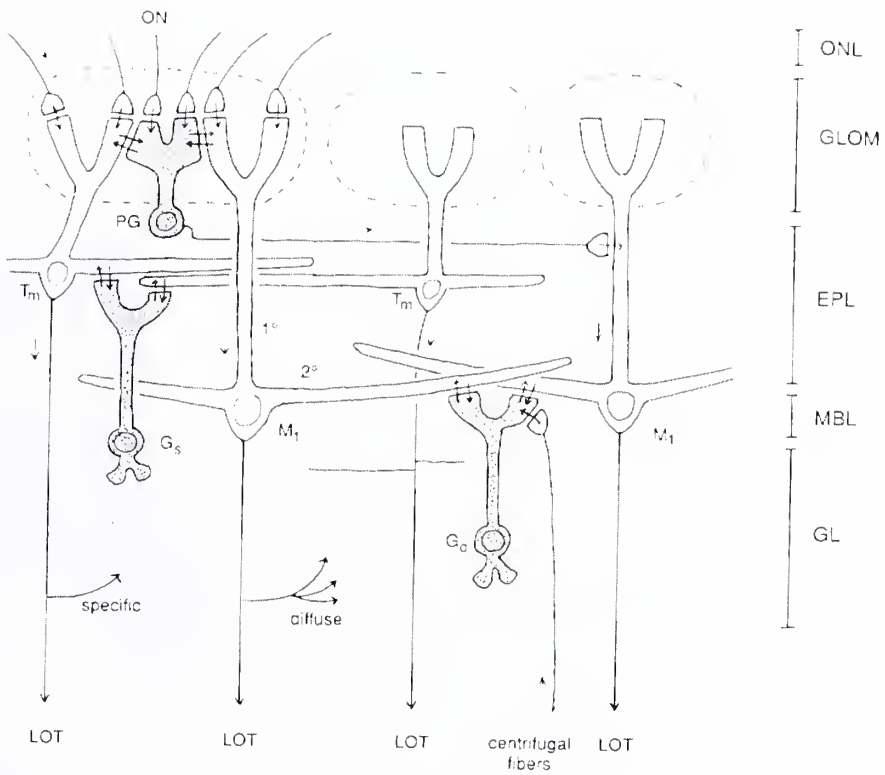
ON
ONL
GLOM
PG
EPL
T_m
T_m
1°
2°
MBL
G_S
M_1
M_1
GL
G_D
specific
diffuse
LOT
LOT
LOT
centrifugal fibers
LOT

Heterogeneity of the Glomerulus

Initially, the glomerulus was perceived as a relatively homogeneous structure in which primary afferent axons and target dendrites were uniformly distributed. However, numerous lines of evidence have suggested that the intrinsic organization of a single glomerulus may exhibit significant complexity and heterogeneity.

Camera lucida reconstructions performed by Halasz and Greer (1993) demonstrated that the terminal arbors of olfactory receptor cell axons are spatially restricted to small areas or subcompartments within an individual glomerulus, suggesting that afferent input to a glomerulus may be spatially segregated. Similarly, Treloar et al. (1996) showed that olfactory receptor cell axons entering a single glomerulus can differentially express cell surface markers such as the lectin Dolichos biflorus. Moreover, these subsets of axons can segregate into different areas of a single glomerulus, supporting the notion that phenotypically distinct subsets of olfactory receptor cells may target the same glomerulus.

Ultrastructural studies of glial processes in the glomerulus have demonstrated two glomerular compartments consisting of a glia-free olfactory receptor cell axon compartment and a dendritic compartment containing glial processes (Chao et al., 1997). The two compartments appeared segregated, in part, by a glial boundary. Additionally, Kosaka et al. (1997) described similar findings showing a differential distribution of periglomerular cell dendrites to different glomerular subcompartments.

These observations support the idea that the mammalian olfactory bulb glomerulus can consist of several different subcompartments that may restrict the distribution of both primary afferents as well as local synaptic circuits. Similar

suggestions have been made based on previous studies in the olfactory lobe of the insect (Boeckh and Tolbert, 1993; Hansson et al., 1991) as well as the crustacean (Schmidt and Ache, 1992).

Development of the Glomerulus

Analyses of the early development of the glomerulus have emphasized the seminal role of primary afferents in inducing the formation of glomeruli (Graziadei and Monti-Graziadei, 1986; Malun and Brunjes, 1996; Valverde et al., 1992; Treloar et al., 1999). In mammals, glomeruli are first apparent during late embryonic development. During the postnatal period glomeruli increase in size and definition with a now general consensus that new glomeruli are not formed de novo beyond postnatal days 2-5 (Meisami and Sendera, 1993).

Functional analyses of olfactory bulb glomeruli using 2-deoxyglucose probes have suggested that mature, adult-like patterns of odor induced activity are not apparent until approximately postnatal week 2. This suggests that while initial glomeruli are present during the early postnatal period, substantial development and maturation continues for a more extended period. This notion is supported by the work of Hinds and Hinds (1976a,b) who demonstrated that synaptogenesis in the olfactory glomeruli of mice continued into postnatal week 2. Similarly, Malun and Brunjes (1996) have shown that the development of dendritic arbors in both the rat and precoccial opposum can continue well into the postnatal period.

Statement of purpose and hypothesis

The purpose of the first study was to explore the cellular and synaptic organization of the olfactory bulb glomerulus and to pursue the hypothesis of a subcompartmental organization. In collaboration with Hahnah J. Kasowski, we examined glomerular organization using confocal microscopy and markers for various cellular components. Immunocytochemistry using olfactory marker protein (OMP), which is specific for olfactory receptor cell axons, and microtubule associated protein (MAP2), which is specific for dendrites, were performed to the assess the distribution of axonal and dendritic processes within the glomerulus. Immunocytochemistry for glial fibrillary acidic protein (GFAP), a marker for glial processes, was employed to assess the distribution of glial processes. The distributions of two synaptic vesicle proteins, synapsin I and synaptophysin, were visualized with immunocytochemistry in conjunction with double labeling studies with OMP and MAP2. To more closely examine the subcompartments identified by the preceding immunocytochemical studies, electron microscopy was utilized. These results have been published as follows:

Kasowski, H., **Kim, H**. and Greer, C. (1999) Compartmental organization of the olfactory bulb glomerulus, The Journal of Comparative Neurology 407: 261-274.

The purpose of the second study, completed as a result of work performed independently, was to gain new insight into the maturation of glomeruli and to better understand the spatio-temporal interactions that occur during postnatal development. We employed confocal microscopy to visualize the organization of immature and mature

olfactory receptor cell axons in parallel with a marker for synaptic specializations in maturing glomeruli to document the emergence of subcompartmental organization in olfactory bulb glomeruli during postnatal development. Rats at postnatal days 1, 6, 12, and 18 were processed for single and double label immunocytochemistry for OMP, used as a marker of mature axons; growth associated protein (GAP-43), used as a marker for immature axons; and synaptophysin, used to distinguish synaptic connections. Light microscopy was also used to visualize cresyl violet stained sections of the olfactory bulb at similar ages. These results have been accepted for publication and the manuscript is in press as follows:

Kim. H. and Greer, C. (2000) The emergence of compartmental organization in olfactory bulb glomerui during postnatal development, The Journal of Comparative Neurology, In Press.

Materials and Methods

ADULTS

Immunocytochemistry

Sprague-Dawley rats (n = 12), 50 - 60 days old, were deeply anesthetized with an intraperitoneal pentobarbital (Nembutal 65mg/kg) and fixed by cardiac perfusion with 0.1M phosphate buffered saline (PBS), pH = 7.2, at 4°C followed by 200-400ml of 4% paraformaldehyde at 4°C. Following perfusion the brains were removed and placed in 4% paraformaldehyde for 1-2 hr at 4°C. Brains were then transferred to 0.1M PBS and stored overnight at 4°C. Sections were cut at 50μm on a vibratome and collected in 0.1M PBS. Sections were either directly processed for immunocytochemistry or were transferred to tissue culture wells containing 30% sucrose for long term storage at 0°C. These stored sections were washed with several rinses of 0.1M PBS before processing for immunocytochemistry.

Following several rinses in 0.1M PBS, sections were preincubated in 0.1M PBS, 1% bovine serum albumen (BSA, Sigma; St. Louis, MO), and 0.2% Triton X-100 for 30 minutes Sections were again rinsed 5 X 5 minutes in 0.1M PBS and then processed individually or sequentially with two of the following primary antibodies: goat anti-olfactory marker protein (OMP) (1:3,000, generously provided by Dr. F. Margolis); mouse anti-microtubule associated protein II (MAP2) (1:500, Sigma; St. Louis, MO); mouse or rabbit anti-synaptophysin (1:100, mouse, ICN Biochemicals; Costa Mesa, CA; 1:100, rabbit, Dako Inc.; Glostrup, Denmark); rabbit anti-synapsin 1 (1:2,000, Signal

Transduction Inc.; San Diego, CA); or rabbit anti-glial fibrillary associated protein (GFAP) (1:2,000, Dako Inc.). Tissue was incubated with the primary antibodies for 24-48 hr at 4°C. Dilutions were made with 0.1M PBS; 0.5% BSA, and 0.2% Triton X-100 was added to the OMP incubation. The protocol for synapsin 1 was as previously described (Mandel et al., 1992) and differs from the above as follows: sections were preincubated for 30 minutes with goat serum dilution buffer (0.45M NaCl, 20mM PB, 17% whole goat serum) and were incubated with the primary antibody, diluted in goat serum dilution buffer, for 4-6 hours. Following primary antibody incubation, sections were rinsed in buffer (0.5M NaCl, 20mM PB, 0.3% Triton X-100). For each single and combination of staining preparations, tissue was processed as a negative control by omitting the primary antibody.

After 5 X 5 minute washes in 0.1M PBS, the sections were incubated with secondary antibodies for 1-2 hours at room temperature. All secondary antibodies were purchased from Vector (Burlingame, CA) and used at 1:100 concentration except where indicated below. Secondary antibodies used were fluorescein horse anti-mouse IgG, texas red horse anti-mouse IgG, texas red donkey anti-goat IgG (Jackson Immunoresearch Laboratory Inc.; West Grove, PA), texas red donkey anti-rabbit IgG (Jackson Immunoresearch Laboratory Inc.; West Grove, PA), fluorescein conjugated AffiniPure donkey anti-rabbit IgG, fluorescein goat anti-rabbit IgG. Dilutions were made with 0.1M PBS, 0.5% BSA except for the synapsin 1-labeled sections for which the secondary antibody was diluted in goat serum dilution buffer. The sections were rinsed in 0.1M PBS and mounted on gelatin-coated slides and coverslipped using Vectashield mounting medium (Vector). Mounted sections were viewed on a Bio-Rad 600 scanning

confocal microscope (Olympus IMT2) equipped with a krypton-argon laser. Images were processed on a Macintosh 7200 computer using Adobe Photoshop (3.0.1) software and printed with a Codonix NP1600M color printer. Image brightness was equalized across panels but further processing was not employed.

Electron Microscopy

Electron microscopy protocols followed those we have previously described (Greer and Hálasz, 1987). Rats were deeply anesthetized as above and subjected to an intracardiac perfusion with 4°C 0.1M PBS followed by 1% glutaraldehyde and 4% paraformaldehyde at 4°C in 0.1M PBS. Olfactory bulbs were dissected and post-fixed in the perfusate overnight. Coronal sections were cut at 100μm on a vibratome and the tissue was osmicated with 2% osmium tetrachloride for 1 hour. A series of graded alcohol washes followed the osmication, beginning with 50% EtOH for 10 minutes and 70% EtOH for 10 minutes. The sections were then stained en bloc with 1% uranyl acetate in 70% EtOH for 1 hour. Alcohol washes continued with 70% EtOH for 10 minutes, 90% EtOH for 10 minutes, three washes of absolute EtOH for 15 minutes each and 2 washes with propylene oxide for 5 minutes each. The sections were then left overnight in a 1:1 propylene oxide/EPON mixture on a shaker. The following day, sections were infiltrated with EPON (EPON 812) for 2 hours, flat-embedded in fresh EPON onto quick-release coated (Hobby Time Mold Parting Compound; Electron Microscopy Sciences, Ft. Washington, PA) slides, coverslipped with quick release coated coverslips and polymerized in a 60°C oven overnight. Slides were examined with a light microscope and following removal from the slide/coverslip, areas of the EPON film

containing tissue of interest were cut out and remounted on EPON blocks for thin sectioning. Blocks were trimmed to ensure that 1 or more glomeruli were within the area being cut and then thin sectioned at 70-100nm, silver sections. Two x 1mm slotted grids covered with formvar (0.5% in ethylene dichloride) were used to collect the sections. The grids were post-stained with 1% lead citrate for 1.5 minutes. A JEOL 1200 EXII 120 kV transmission electron microscope was used for the microscopic/photographic analysis of the tissue.

Electron micrograph montages of individual glomeruli were collected at 800X and, following printing at a final magnification of 2,080X, were used to assess the area (μm^2) occupied by ORC axons within the glomerulus. The individual electron micrographs were combined to make a montage that included an entire glomerulus in cross section. The axonal areas, which can be distinguished from dendritic areas due to their relative electron density, were then outlined in pen to readily distinguish them from apposed dendritic areas. Planimetry was employed to establish the area (μm^2) of the glomerulus and the area (μm^2) occupied by the axonal profiles within the glomerulus. The perimeter of the glomerulus was defined by surrounding juxtaglomerular cells.

To examine the synaptic specializations within the glomerulus, columns or rows of overlapping electron micrographs, probes, that passed through the height or width, respectively, of the glomerulus were collected at 12,000X and printed at 30,000X. These micrographs were then montaged together such that a reconstructed probe through one glomerulus was typically more than six feet in length. All of the synapses within a probe were highlighted and then identified as being axodendritic, dendrodendritic mitral/tufted to periglomerular cell, or dendrodendritic periglomerular to mitral/tufted cell. The type

and orientation of the synapses was clearly distinguishable in approximately 70% of synapses due to differences in synaptic vesicle morphology or the appearance of the synaptic membrane specializations (vide infra). It was not possible to consistently distinguish whether the postsynaptic process in axodendritic connections was from a mitral/tufted or periglomerular cell because the synaptic specializations are identical.

In order to test the hypothesis that primary afferent synapses are located at more distal sites on dendritic processes relative to local circuit or dendrodendritic synapses which may be found more proximally, we measured the cross sectional diameters of mitral/tufted dendritic processes that were postsynaptic to periglomerular cells or dendrites postsynaptic to ORC axons. In total, 200 dendrites receiving dendrodendritic synapses and 200 dendrites receiving axodendritic synapses were measured. The cross sectional dendritic diameter was determined in each case by measuring the dendrite in both the perpendicular and parallel planes relative to the postsynaptic specialization.

DEVELOPMENTAL

Animals

All protocols and animals used were reviewed and approved by the Yale Animal Care and Use Committee. Sprague-Dawley rats, postnatal day 1 (n=4), 6 (n=4), 12 (n=4), and 18 (n=5), were deeply anesthetized with an intraperitoneal injection of pentobarbital (Nembutal 65 mg/kg) and perfused through the heart with 0.1M phosphate buffered saline (PBS) (pH=7.4) at 4°C followed by 100-200 ml of 4% paraformaldehyde in 0.1M PBS at 4°C. The brains were then removed and immersed in 4% paraformaldehyde for 1-2 hours at 4°C before washing in 0.1M PBS for 24 hours at 4°C. The olfactory bulbs were then embedded in 2% agar and coronal sections cut at 50μm on a vibratome. The sections were collected in a cryoprotectant, 30% sucrose, for storage at -20°C prior to processing for immunocytochemistry.

Alternatively, Sprague-Dawley rats at postnatal days 0 (n=2), 6 (n=2), 12 (n=2) and 18 (n=2) were processed for paraffin embedding following perfusion and dissection as described above. The olfactory bulbs were cut at 10 μm in the coronal plane and stained with thionine for histological analysis.

Immunocytochemistry

Selection of Antibodies

To identify mature olfactory receptor cell axons we employed anti-olfactory marker protein (OMP). OMP is a cytoplasmic protein that is highly specific to the majority of olfactory receptor cell axons in the olfactory bulb (Ring et al., 1997;

Margolis, 1985; Monti-Graziadei et al., 1980) and upregulates as the axons mature and establish synapses (Verhaagen et al., 1989, 1990). Although some populations of OMP expressing cells are found outside of the olfactory bulb (Baker et al., 1989), these are unlikely to compromise the analyses because they do not project processes to the olfactory bulb glomeruli. To identify immature olfactory receptor cell axons we employed anti-growth associated protein-43 (GAP-43). GAP-43 is a membrane associated protein found in growing immature axons (Meiri et al., 1988) and is abudantly expressed in immature olfactory receptor cell axons prior to the appearance of OMP (Verhaagen et al., 1989, 1990; Gong and Shipley, 1995; Treloar et al., 1996). It is important to note that GAP-43 expression is not limited to olfactory receptor cell axons, it may also be expressed in juxtaglomerular cells and centrifugal axons during development. However, because the majority of staining appears in olfactory receptor cell axons and because contributions from other cell populations are transient, GAP-43 proved to be the most effective marker of developing olfactory receptor cell axons. Finally, anti-synaptophysin was employed as a marker for the presence of synaptic vesicles (Jahn and Sudhof, 1994). While not a definitive measure of synapse formation, synaptophysin staining does establish the presence of a synaptic vesicle associated protein and has been effectively employed to determine the appearance (Johnson et al., 1996) and distribution (Kasowski et al., 1999) of synapses in the olfactory bulb glomerulus as well as elsewhere in the CNS (e.g. Tyzio et al., 1999).

Staining Protocol

The protocol for immunocytochemistry was described previously (Kasowski et al., 1999). Briefly, the tissue sections stored at -20°C were washed with several rinses of

0.1M PBS before processing for immunocytochemistry. All immunocytochemical reactions were performed on free floating sections. Following 2×10 minute rinses in 0.1M PBS, sections were preincubated in 0.1M PBS with 1% bovine serum albumin (BSA, Sigma Chemical Co.) and 0.2% triton X-100 (Sigma Chemical Co.) for 30 minutes at room temperature. Sections were then rinsed 5×7 minutes in 0.1M PBS with 0.5% BSA at room temperature before incubating for 24-48 hours at 4°C in one of the following antibodies: goat anti-OMP (1:1000, generously provided by Dr. F. Margolis); rabbit anti-synaptophysin (1:100, Dako Co.); mouse anti-GAP-43 (1:500, Boehringer Mannheim). Dilutions were made in 0.1M PBS with 0.5% BSA. Sections were then rinsed 5×7 minutes in 0.1M PBS with 0.5% BSA before incubating for 1 hour at room temperature in one of the following secondary antibodies: rhodamine (TRITC)-conjugated AffiniPure donkey anti-goat IgG (H+L) (Jackson ImmunoResearch Labs, Inc.); fluorescein goat anti-rabbit IgG (H+L); Texas red goat anti-rabbit IgG (H+L) (1:200); fluorescein horse anti-mouse IgG (H+L), rat adsorbed. All secondary antibodies were purchased from Vector Labs, Inc. and used at a concentration of 1:100, except where noted above. Processing was then repeated as above using a second set of primary and secondary antibodies before mounting on precleaned slides and coverslipping with Vectashield mounting medium (Vector Labs, Inc.). The sequence in which the primary antibodies were used in the double labeling studies was varied to ensure that the patterns of labeling did not reflect the processing sequence.

Controls

To control for non-specific and artifactual staining, the primary antibodies were excluded in a series of experiments at each of the ages. In all cases, staining did not occur in the absence of the primary antibody.

Light and Confocal Microscopy

The cresyl violet stained sections were assessed on an Olympus BH2 microscope and representative images were captured at 1200 dpi into Adobe Photoshop using a Spot Camera (Diagnostic Instruments Inc., Sterling Heights, MI).

Mounted sections processed for immunocytochemistry were visualized and images were collected using a Bio-Rad 600 scanning confocal microscope (Olympus IMT2) equipped with a krypton-argon laser. The average thickness of optical sections from which images were obtained was approximately 1.0μm. Serial reconstructions were used to evaluate multiple images viewed through the depth of a tissue sample. To minimize regional differences in the organization (e.g. Ring et al., 1997) or maturation (e.g. Bailey et al., 1999) of the olfactory bulb, data acquisition and analysis focused on sections taken from midway along the rostral-caudal axis. To ensure that the edges of glomeruli were not misinterpreted as sections passing through the center of a glomerulus, all glomeruli included in the analyses and used for illustration in the manuscript were at least partially viewed through serial optical sections on the confocal microscope. The magnifications used in all of the illustrations were selected to emphasize the features of interest for each of the antibodies at each of the representative ages.

A Macintosh 7200 computer equipped with Adobe Photoshop (3.0.1) software was used to format and present the images, which were printed on a Codonix NP1600M color printer. Image brightness and contrast were balanced for consistency within a figure, but further processing was not performed on any of the images.

Results

ADULTS

Increasing evidence indicates that the olfactory bulb glomerulus serves as a fundamental organizational unit for odor representation. Activity mapping studies with 2-deoxyglucose (2DG) demonstrated that specific odorants elicited spatially defined patterns of glomerular activity in the olfactory bulb (Greer et al., 1982; Jourdan et al., 1980; Lancet et al., 1982; Stewart et al., 1979). Similar results have been obtained by using cFOS immunocytochemistry (Guthrie et al., 1995; Onoda, 1992; Sallaz and Jourdan, 1993). Electrophysiological studies have further demonstrated that the mitral cells associated with individual glomeruli are differentially responsive or "tuned" to specific odorants (Buonviso and Chaput, 1990; Mori et al., 1992). These functional analyses are consistent with the recent demonstration that axons from olfactory receptor cells (ORC) expressing the same odor receptor converge onto only two or a few glomeruli in the olfactory bulb (Mombaerts et al., 1996; Ressler et al., 1994; Vassar et al., 1994).

The glomerulus is a complex and well delineated neuropil that is the site of the first synapse in the olfactory pathway (for reviews see: Shepherd and Greer, 1998; Shipley and Ennis, 1996). The spherical or ovoid glomeruli are defined by glial wrappings and surrounding somata of peri/juxtaglomerular cells. Within glomeruli dense networks of ORC axons make excitatory synapses onto the dendritic processes of projection neurons, mitral and tufted cells, and local circuit interneurons, periglomerular

cells. The dendritic processes interact via reciprocal dendrodendritic synapses which modulate intraglomerular processing of odor. While glomerular synapse structure has not yet been fully characterized, it is interesting to note the unusually high concentrations of at least one synaptic vesicle associated protein, synapsin 2, in olfactory receptor cell axon terminals (Stone et al., 1994).

Despite the recent emphasis on the functional and structural homogeneity of individual glomeruli, several alternative lines of evidence have suggested that the intrinsic organization of single glomeruli can be very complex. Hálasz and Greer (1993) showed that the terminal arbors of ORC axons are spatially restricted to small areas or subcompartments within a glomerulus suggesting that afferent input to a glomerulus may be heterogeneous or spatially segregated. Similarly, Treolar et al. (1996) showed that ORC axons entering a single glomerulus can differ in their expression of cell surface markers such as the lectin *Dolichos biflorus* and moreover, that these subpopulations of axons can segregate into different areas of a single glomerulus. In a related context, Johnson et al. (1996) noted that intraglomerular immunoreactivity for synaptophysin was most dense along the periphery of glomeruli, proximal to the olfactory nerve layer, suggesting that synapses may be heterogeneously distributed within glomeruli.

Chao et al. (1997), in ultrastructural studies of glial processes in the glomerulus, identified two glomerular compartments: 1) a glial free ORC axon compartment; and 2) a dendritic compartment that contained glial processes. The two compartments appeared segregated, in part, by a glial boundary. Recently, Kosaka et al. (1995, 1997) reported similar findings on the segregation of periglomerular cell dendrites to different glomerular compartments. Periglomerular cell dendrites that were immunoreactive for

anti-calbindin were restricted to the dendritic compartments while those immunoreactive for either gamma aminobutyric acid (GABA) or tyrosine hydroxylase were uniformly distributed throughout the glomerulus. Consistent with the differential distribution of calbindin immunoreactive processes, Toida et al. (1998) reported that this subpopulation of periglomerular cell dendrites received almost no synaptic input from ORC axons. These recent observations appear consistent with the notion that the mammalian glomerulus can be composed of several subcompartments that may restrict the distribution of subsets of primary afferents as well as segregating primary afferent and local synaptic circuits. Such an organization has been previously described in the olfactory lobe of both the insect (Boeckh and Tolbert, 1993; Hansson et al., 1991) as well as the crustacean (Schmidt and Ache, 1992).

The purpose of the current study was to explore further the synaptic organization of olfactory bulb glomerular compartments. The data demonstrate that the glomerulus is a complex heterogeneous structure. Primary afferent synapses are restricted to axonal compartments while dendrodendritic local circuit synapses occur predominately in dendritic compartments that are delineated in part by glial processes. These results support the hypothesis of a subcompartmental organization within olfactory bulb glomeruli.

Characterization of Axonal and Dendritic Processes By OMP, MAP2 and GFAP Immunoreactivity

OMP and MAP2

As is well known, OMP immunoreactivity (OMP-IR) identifies ORC axons in the olfactory bulb (Margolis, 1972). OMP-IR was densely distributed in the olfactory nerve layer and glomerular layer of the olfactory bulb (Figure 3A). Fascicles expressing OMP-IR were evident exiting the olfactory nerve layer to enter individual glomeruli (i.e. Figure 3A, arrowhead). Upon entering the glomerulus the fascicles dissociated into islands of dense OMP-IR alternating with areas devoid of OMP-IR. Because the islands of OMP-IR were larger in diameter than single ORC axons (~0.2μm) it seems likely that these islands represent conglomerations of axons and/or terminal enlargements (cf. Figure 5).

Because OMP-IR left adjacent areas in the glomerular neuropil unstained, we used MAP2-IR to assess the distribution of dendritic processes within the glomerulus. MAP2 is associated with cytoskeletal elements found specifically in dendrites (Caceres et al., 1986) and is effective in identifying the dendritic constituents of glomeruli (Philpot et al., 1997). MAP2-IR was evident in the external plexiform and glomerular layers of the olfactory bulb; no MAP2-IR was found in the olfactory nerve layer (Figure 3B). In the external plexiform layer both radially and horizontally stained processes were present. Emerging from the dense staining of the external plexiform layer were individual radially oriented processes that arborized into progressively smaller branches after entering glomeruli. Surrounding the glomeruli and within the external plexiform layer non-IR somata of juxtaglomerular neurons were evident. The distinct MAP2-IR processes extending from the external plexiform layer to the glomerular layer to enter individual glomeruli seem most likely to represent the apical dendrites of mitral and tufted cells. The dendritic processes emanating from the population of juxtaglomerular neurons are less evident because of their smaller size and because they arborize immediately at the

Figure 3 : Confocal images, reconstructed from serial optical planes, of OMP, MAP2, synaptophysin, or synapsin 1 immunoreactivity (IR) in the superficial layers of the olfactory bulb. (A) OMP-IR shows the distribution of olfactory receptor cell axons within the olfactory nerve layer and glomerular layer. Arrowheads indicate the fascicles of ORC axons approaching the glomerulus. Upon entering the glomerulus the fascicles dissociated into islands of dense OMP-IR alternating with areas devoid of IR. (B) MAP2-IR is associated with dendritic processes in the glomerular layer and external plexiform layer. Individual dendrites, indicated by arrowheads, are shown emerging from the dense staining of the external plexiform layer and traveling to individual glomeruli were they then arborized into progressively smaller branches. (C) A punctate pattern of synaptophysin immunoreactivity is found throughout the glomerulus as well as in the external plexiform layer. Synaptophysin-IR was not evident in the olfactory nerve layer and only rarely seen juxtaglomerularly in the glomerular layer. Within the glomerulus synaptophysin-IR is heterogeneous in that there appear zones that are more densely IR. The glomerular pattern of synapsin 1-IR (D) was generally similar to that of synaptophysin although the synapsin 1-IR puncta were more granular in appearance and the overall IR appeared more diffuse. Also in contrast to synaptophysin, significant staining was seen in the juxtaglomerular zone between glomeruli. Abbreviations: OMP-IR, olfactory marker protein immunoreactivity; MAP2, microtubule associated protein 2; ONL, olfactory nerve layer; GLL, glomerular layer; EPL, external plexiform layer.

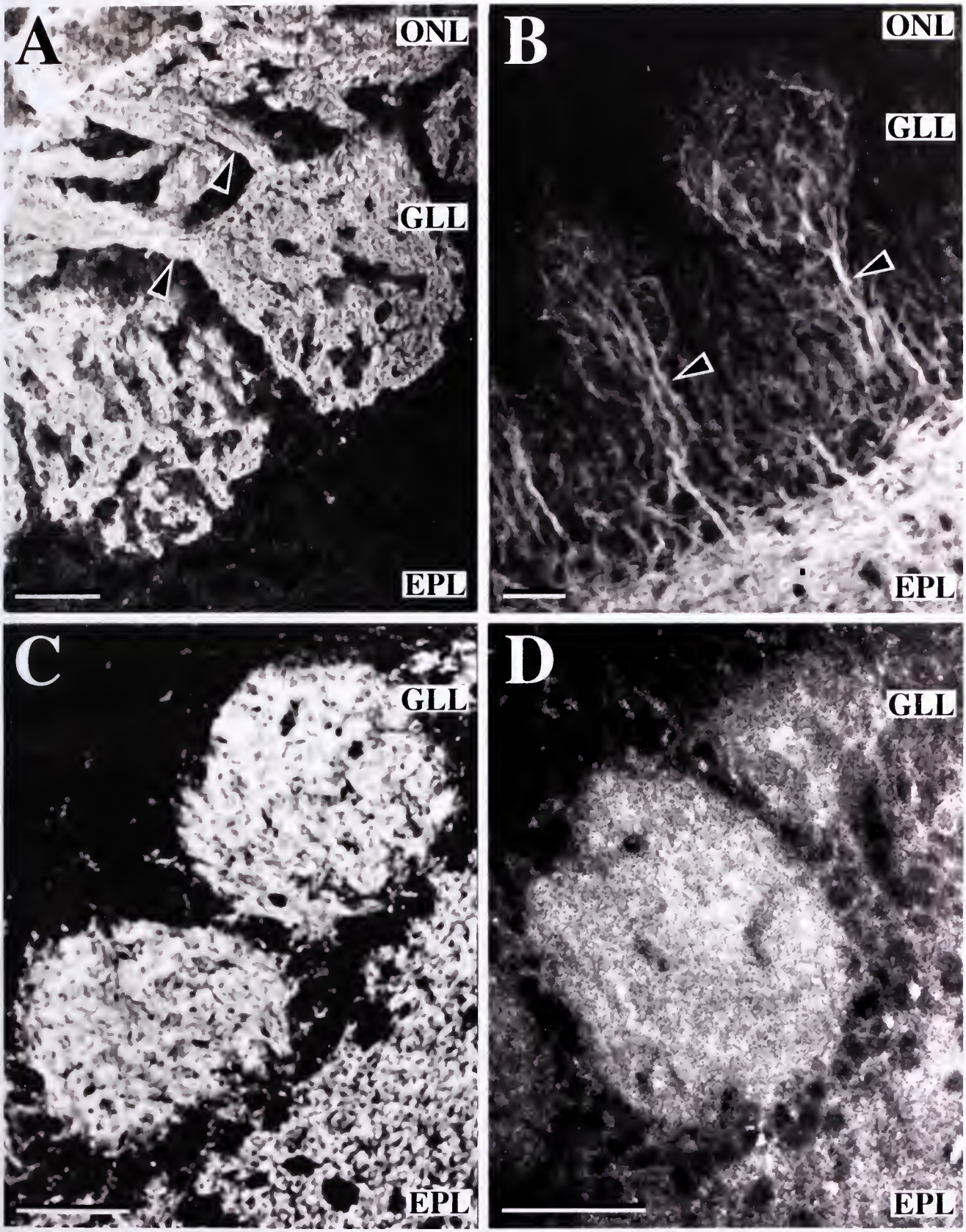
A
ONL
GLL
EPL
B
ONL
GLL
EPL
C
GLL
EPL
D
GLL
EPL

Figure 4: Confocal images, reconstructed from serial optical planes, of combinations of OMP, MAP2, GFAP, synaptophysin, and synapsin 1 IR. (A,B) OMP-IR and MAP2-IR are seen to occupy distinct areas within the glomerulus. OMP-IR axonal processes (green) are seen distributing into islands of dense IR indicated by arrowheads. Individual dendritic processes (red; i.e., arrows) interdigitate between the OMP-IR with minimal colocalization. (C) OMP (green; i.e., arrow) and GFAP-IR (red/yellow; i.e., arrows), which identifies glial processes, are shown. Note how the glial processes appear to dissect between OMP islands being primarily associated with non-OMP areas. (D, E) Doubled-labeled preparations with synaptophysin and OMP (D) or MAP2 (E). In (D) extensive colocalization (yellow; i.e., arrowheads) is apparent between synaptophysin-IR (red) and OMP-IR (green). At the upper left in (D) an OMP-IR fascicle, indicated by an arrow, is seen entering the glomerulus. Asterisks in (D) indicate areas of synaptophysin-IR (red) between areas of OMP-IR. Small puncta of individual OMP-IR and synaptophysin-IR were seen interspersed among colocalizing areas. In contrast, note the relative paucity of colocalization in MAP2-IR (red) and synaptophysin-IR (green) shown in (E). Individual dendrites entering the glomerulus from the EPL, labeled by MAP2, are indicated by arrows in (E). (F, G) Double-labeled preparations with synapsin 1 and OMP (F) or MAP2 (G) are shown. OMP-IR (green; i.e., arrowheads) and synapsin 1-IR (red; i.e., asterisks) appeared largely distinct. While evidence of colocalization was seen, it was less robust than that seen with OMP/synaptophysin-IR or MAP2/synapsin 1-IR. (G) Synapsin 1-IR (red) colocalized strongly with MAP2-IR (green). In (G) it is notable that the areas of colocalization (yellow-orange) appear as well defined processes (i.e., arrows) as was seen in the MAP2-IR alone. Abbreviations: OMP-IR, olfactory marker protein immunoreactivity; MAP2, microtubule associated protein 2; GFAP, glial fibrillary associated protein; ONL, olfactory nerve layer; GLL, glomerular layer; EPL, external plexiform layer.

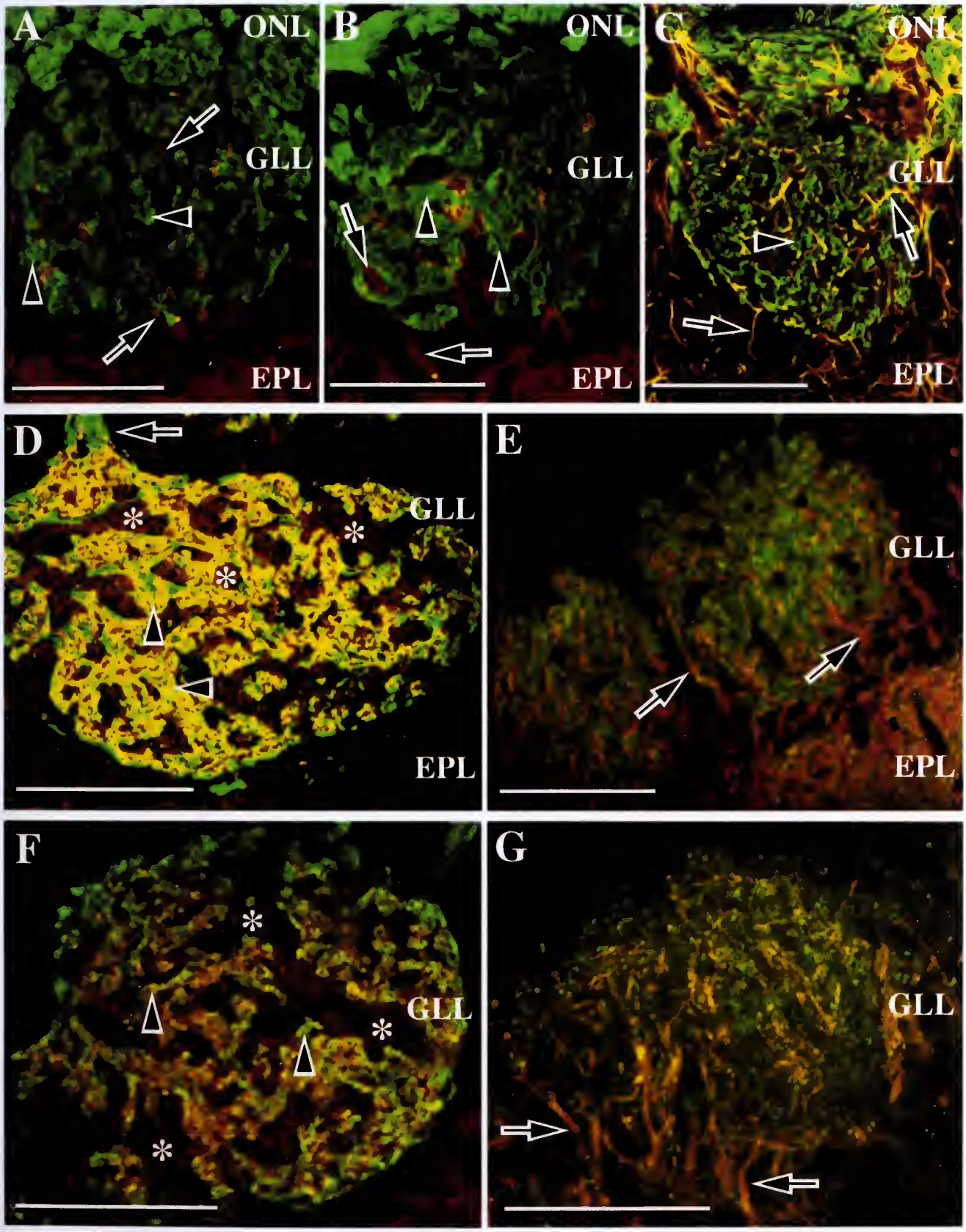
A
ONL
GLL
EPL
B
ONL
GLL
EPL
C
ONL
GLL
EPL
D
GLL
EPL
E
GLL
EPL
F
GLL
G
GLL

border of the glomerulus.

To explore the interaction of ORC axons and dendritic processes within the glomerular neuropil tissue sections were double labeled using FITC and Texas Red secondary antibodies, respectively. The double labeling demonstrated that OMP-IR and MAP2-IR occupied distinct areas within the glomerulus. In Figure 4A,B OMP-IR axonal processes (green) are seen distributing in a pattern equivalent to that seen with OMP-IR alone (cf. Figure 3A). The areas of MAP2-IR dendritic processes (red) interdigitate between the distinct islands of predominately OMP-IR. In those areas where a suggestion of co-localization is seen (yellow) it most likely reflects tightly apposed or overlapping axonal and dendritic processes within the optical section and not the presence of both epitopes in a single process. Within the islands of OMP-IR there were puncta of MAP2-IR that may be suggestive of single or small groups of dendritic processes (cf. Figure 4D). In contrast, the areas of MAP2-IR did not show evidence of OMP-IR puncta.

GFAP

To further characterize the cellular elements comprising a glomerulus we used glial fibrillary acidic protein immunoreactivity (GFAP-IR) to visualize the glial processes (cf. Bailey and Shipley, 1993; Chiu and Greer, 1996). GFAP-IR processes were observed throughout the olfactory nerve layer, glomerular layer, and external plexiform layer. IR was intense in the olfactory nerve layer as bundles of ORC axons appeared ensheathed in dense glial processes, as has been previously described at the ultrastructural level (Doucette, 1993). In sections double labeled for GFAP-IR (red) and

border of the glomerulus.

To explore the interaction of ORC axons and dendritic processes within the glomerular neuropil tissue sections were double labeled using FITC and Texas Red secondary antibodies, respectively. The double labeling demonstrated that OMP-IR and MAP2-IR occupied distinct areas within the glomerulus. In Figure 4A,B OMP-IR axonal processes (green) are seen distributing in a pattern equivalent to that seen with OMP-IR alone (cf. Figure 3A). The areas of MAP2-IR dendritic processes (red) interdigitate between the distinct islands of predominately OMP-IR. In those areas where a suggestion of co-localization is seen (yellow) it most likely reflects tightly apposed or overlapping axonal and dendritic processes within the optical section and not the presence of both epitopes in a single process. Within the islands of OMP-IR there were puncta of MAP2-IR that may be suggestive of single or small groups of dendritic processes (cf. Figure 4D). In contrast, the areas of MAP2-IR did not show evidence of OMP-IR puncta.

GFAP

To further characterize the cellular elements comprising a glomerulus we used glial fibrillary acidic protein immunoreactivity (GFAP-IR) to visualize the glial processes (cf. Bailey and Shipley, 1993; Chiu and Greer, 1996). GFAP-IR processes were observed throughout the olfactory nerve layer, glomerular layer, and external plexiform layer. IR was intense in the olfactory nerve layer as bundles of ORC axons appeared ensheathed in dense glial processes, as has been previously described at the ultrastructural level (Doucette, 1993). In sections double labeled for GFAP-IR (red) and

OMP-IR (green) (Figure 4C) glial processes within the glomerulus appeared to follow tortuous courses as they interdigitated with the islands of OMP-IR. Areas of apparent colocalization of GFAP and OMP (yellow in Figure 4C) represent superimposed processes as well as some bleed through from the GFAP secondary antibody and not colocalization of the epitopes in the same process.

Characterization Of Glomerular Synaptic Vesicle Associated Proteins

Synaptophysin

Several recent studies have used antibodies for synaptic vesicle associated proteins to visualize sites of synaptic specializations and to identify subpopulations of synapses based on differences in their associated vesicle proteins. Synaptophysin is an integral protein of the synaptic vesicle membrane and is thought to be involved in the formation of an exocytotic fusion pore during vesicle release (Jahn et al., 1985; Thomas et al., 1988). As seen in Figure 3C, a punctate pattern of synaptophysin IR is found throughout the glomerulus as well as in the external plexiform layer. Synaptophysin-IR was not evident in the olfactory nerve layer. Within the glomerulus it is clear that synaptophysin-IR is heterogeneous in that there appear zones, particularly around the glomerular border proximal to the olfactory nerve layer, that are more densely IR. The juxtaglomerular zones surrounding the glomeruli are largely devoid of synaptophysin-IR. Thus, the glomeruli appear very well demarcated as spheres of synaptophysin-IR. The small spherical areas within the glomeruli and external plexiform layer that are devoid of IR most likely correspond to juxtaglomerular cell bodies or blood vessels.

To establish the cellular localization of synaptophysin-IR, double labeling was performed with anti-OMP or anti-MAP2. There was extensive colocalization of synaptophysin-IR and OMP-IR (Figure 4D). In Figure 4D, a fascicle that is only OMP-IR is seen entering the glomerulus (arrow). Within the glomerulus much of the IR is yellow indicating a colocalization of the OMP-IR (green) and the synaptophysin-IR (red). Punctate areas of synaptophysin-IR alone were seen interdigitating among the islands of OMP-IR/synaptophysin-IR. In addition, within the islands of co-localization there was evidence of smaller puncta that were IR for either synaptophysin or OMP alone. Finally, while much of the OMP-IR appears co-localized with synaptophysin-IR, there were also OMP-IR alone regions that helped define the perimeter of the glomerulus.

In contrast to the extensive co-localization of synaptophysin/OMP-IR, synaptophysin/MAP2-IR preparations demonstrated less intense co-localization. In Figure 4F synaptophysin-IR is seen diffusely throughout the glomerulus (cf. Figure 3C). MAP2-IR dendrites (red), seen entering from the external plexiform layer and arborizing within the glomerulus, do not heavily co-express synaptophysin-IR (yellow).

Synapsin 1

Synapsin 1 is also an integral membrane protein of small synaptic vesicles. It binds the actin cytoskeleton and is thought to regulate neurotransmitter release by controlling the number of vesicles available for exocytosis (Bahler et al., 1990; Südhof et al., 1989). Stone et al. (1994) demonstrated that the synapsins have a differential distribution across the olfactory bulb. Synapsin 1 immunoreactivity was found to be

especially intense in the external plexiform and glomerular layers which suggested that synapsin 1 may be preferentially associated with dendrodendritic synapses.

Synapsin 1-IR, like synaptophysin-IR, was found throughout the glomerulus and in the external plexiform layer (Figure 3D). The glomerular pattern of IR was generally similar to that of synaptophysin although the synapsin-IR puncta were more granular in appearance and the overall IR appeared more diffuse. Synapsin 1-IR was also more apparent than synaptophysin in the juxtaglomerular zone between glomeruli and appeared to demarcate the cytoplasm surrounding the nucleus of juxtaglomerular somata.

In double labeled preparations, synapsin 1-IR (red) strongly colocalized with MAP2-IR (green) (Figure 4G). It is notable that the areas of colocalization (yellow-orange) appear as well defined processes as was seen in the MAP2-IR alone (cf. Figure 3B). The MAP2/synapsin 1-IR colocalization appears superimposed on a background of granular appearing synapsin 1-IR alone. While evidence of colocalization was apparent in double labeled preparations with OMP and synapsin 1, (Figure 4F), it was less robust than that seen with OMP/synaptophysin-IR or MAP2/synapsin 1-IR. Synapsin 1-IR is seen between the larger islands of OMP-IR. Puncta of synapsin 1-IR are also observed within the OMP-IR areas, however synapsin 1 and OMP did not exhibit the robust colocalization seen with OMP and synaptophysin.

Ultrastructural Characterization of the Olfactory Bulb Glomerulus

EM preparations of the olfactory bulb glomerulus were used to determine whether the synaptic circuits of the glomerulus were compartmentalized as suggested by the immunocytochemistry preparations. Figure 5A is a montage of electron micrographs that

Figure 5: A glomerulus in cross section constructed from a montage of electron micrographs. The perimeter of the glomerulus is lined by juxtaglomerular cell bodies (i.e., arrows; nuclei outlined in pen). In (A) a fascicle of ORC axons is seen entering the glomerulus from the upper left. Within the glomerulus, axonal islands (i.e., arrowheads), which are characterized in part by their relative electron density, were outlined in pen to more readily distinguish them from adjacent dendritic areas. Note the similarity to immunocytochemistry preparations where axonal subcompartments are seen to interdigitate with non-axonal or dendritic areas. The inset (B) at top right shows a high magnification view of olfactory receptor cell axon terminals making Gray Type 1 synapses (i.e., arrows) onto a dendritic process. Note the differences in electron density between dendrites and axons as well as the high packing density of vesicles within the axon terminals. Blood vessels (i.e., asterisks) were also seen in the glomerular layer. Abbreviations: D, dendrite; Ax, axonal terminal; AF, axon fascicle. Calibration Bars, A = 25μm; B = 0.5μm.

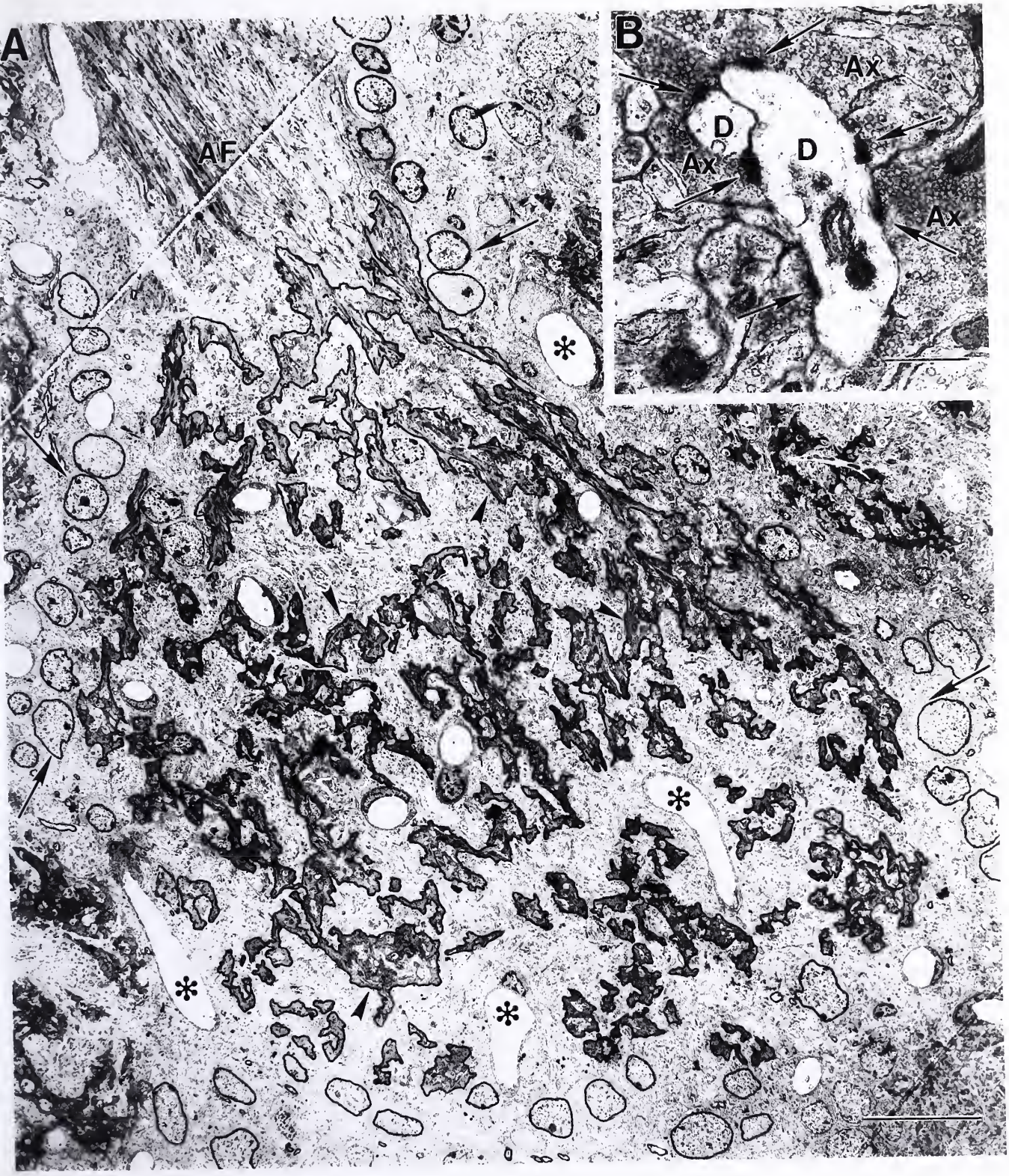
A
AF
B
Ax
D
D
Ax
Ax

covers a single olfactory bulb glomerulus whose perimeter is defined by juxtaglomerular cell bodies. As has been previously noted (Pinching and Powell, 1972), ORC axons and terminals are relatively electron dense and can be distinguished from the electron lucent dendritic processes (Figure 5B). In Figure 5A a large fascicle of ORC axons is seen entering the glomerulus from the olfactory nerve layer. The fascicle, in which the axons are initially tightly apposed, disperses upon entering the glomerulus into smaller bundles of axons which interdigitate among electron lucent dendritic areas. This is reminiscent of the immunocytochemistry preparations where OMP-IR, which localizes to axons, was located throughout the glomerulus in islands that interdigitated with MAP2-IR, which visualizes dendritic processes. Blood vessels, which are seen as white areas devoid of cellular material (asterisk), are also seen dispersed throughout the glomerulus.

Eleven glomeruli were reconstructed at 12,000X as shown in Figure 5. Using the juxtaglomerular neurons as the defining border, these glomeruli had a mean area of 9,715.54 +/- 1,682.42 μm^2. Cumulative analyses of those olfactory nerve terminals that were easily identified within these glomeruli (i.e. Figure 5) showed a mean area of 2,770.17 +/- 493.61μm^2. Because it seems unlikely that we successfully measured all of the olfactory nerve terminals within the glomeruli, we conservatively estimate that ORC axons occupied approximately 28% of the glomerular area.

Both the immunocytochemical analyses and low magnification EM led to the hypothesis that axonal and dendritic compartments could be segregated within the glomerulus. To test this hypothesis, glomeruli were examined at higher magnification, where the primarily axonal and dendritic compartments were easily distinguishedwithin

Figure 6: High magnification electron micrographs of the rat olfactory bulb glomerulus. (A) Cluster of four dendritic processes, most likely from mitral and tufted cells (MT), is surrounded by axonal processes. Several axodendritic synapses are indicated by arrows. These synapses are characterized by numerous round vesicles in the presynaptic specialization and a thick, asymmetrical opposing membrane on the postsynaptic dendrite. Within the glomerulus distinct axonal and dendritic areas could be differentiated. Dendritic areas were often seen to be circumscribed from axonal areas by glial processes (B, C). (B) Long, slender glial process (arrowheads) can be seen dissecting between the dendritic area (Den) below and the axonal area (Ax) above. A smaller dendritic bundle is seen in (C). Linear arrays of intermediate filaments, highly characteristic of glial cells, are indicated by arrowheads in (C). In (D), a mitral/tufted cell process is shown making a dendrodendritic synapse (arrow) onto a periglomerular cell dendrite (PG). Mitral/tufted cells have uniform small, round vesicles that are presynaptic to an asymmetric membrane thickening as is seen in axodendritic synapses. The reciprocal periglomerular cell to mitral/tufted cell dendrodendritic synapse is shown in E, which is an enlargement from B. Periglomerular cells have numerous pleomorphic vessels that are round or oval and are generally larger than those seen in the mitral/tufted cells. The periglomerular to mitral/tufted dendrodendritic synapse can be differentiated from the other pictured synapses by characteristic symmetrical pre- and postsynaptic membrane thickenings. Additionally, dendritic processes receiving dendrodendritic synapses were found to have a significantly larger mean diameter than those receiving axodendritic synapses. This difference is apparent in Figure 4B where dendritic processes in a dendritic subcompartment (Den) can be contrasted with those in an axonal subcompartment (Ax). Note that there are many dendritic processes that have a relatively large diameter in the dendritic subcompartment whereas the individual dendrites in the axonal area (d) are smaller. Abbreviations: Ax, olfactory receptor cell axon; Den, dendrite; MT, mitral/tufted cell dendrite; PG, periglomerular cell dendrite. Calibration Bars, A, C, D and E = 0.5μm; B = 1.0μm.

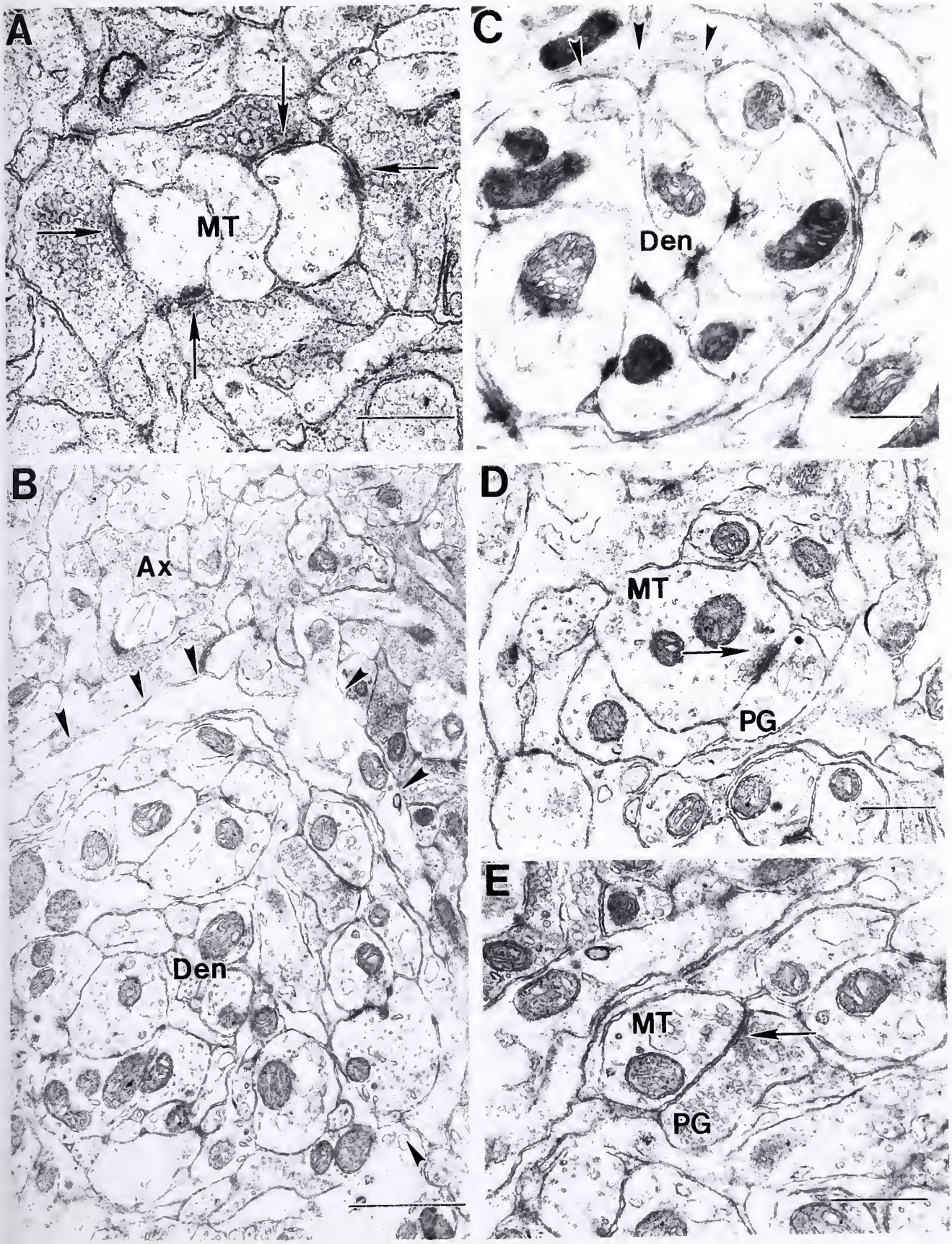
A
MT
C
Den
B
Ax
Den
D
MT
PG
E
MT
PG

the glomerular neuropil (Figure 6A,B,C). In the axonal compartment ORC axons were readily recognized due to the electron dense appearance of the axons and terminal boutons (Figure 6A, cf. 6B). The axons characteristically had abundant, uniform spherical vesicles which appeared to be organized in a matrix that filled the axoplasm. Interspersed among the axon terminals were single or small clusters of dendritic processes that were often postsynaptic to the ORC axons (vide infra). In Figure 6A axonal processes are seen surrounding and making axodendritic Gray Type 1 synapses (arrows) onto a cluster of four dendritic processes that most likely come from mitral/tufted and/or periglomerular cells. Beyond the spherical vesicles noted above, these synapses were also characterized by the thick, asymmetrical membrane on the postsynaptic dendrite. While some dendrodendritic synapses among the small clusters of dendrites were noted within the islands of axonal processes, these were rare relative to the abundant axodendritic synapses found within axonal compartments, as was also observed by Chao et al. (1997). Of further interest, dendroaxonic synapses from mitral/tufted or periglomerular cells onto ORC axons were not observed.

The dendritic compartments that interdigitated with the islands of ORC axons had clusters of dendrites ranging from five to more than a hundred processes. Though this represented a continuum from the number of dendritic processes that were grouped together within the axonal islands, these larger dendritic compartments appeared distinct from the smaller clusters in the patterns of synaptic interactions that were observed. The individual or small groups of dendrites located within the axonal areas were, as reported above, often postsynaptic to axonal processes. Axodendritic synapses were noted at the interface between axonal areas and the larger dendritic compartments, however, the

dendritic compartments showed a preponderance of dendrodendritic synapses. Moreover, no ORC axons, individually or in small groups, were noted within the dendritic areas. Furthermore, the dendritic compartments were often separated from adjacent axonal islands by glial processes (Figures 6B,C). Figure 6B shows the sinuous, slender process of a glial cell encircling a bundle of dendrites, separating them from the relatively electron dense axonal area seen above. In Figure 6C, a smaller bundle of dendrites is shown circumscribed by a glial process in which a bundle of intermediate filaments, characteristic of glial cells, is apparent.

Within the dendritic compartment, dendrodendritic synaptic interactions were abundant. Mitral/tufted and periglomerular cells were identified based on differences in their synaptology and the appearance of their profile as has been previously described (Pinching and Powell, 1971; White, 1973). Mitral/tufted cells have uniform small, round vesicles that were presynaptic to an asymmetrical membrane thickening, a Gray Type 1 synapse. The periglomerular cells have more numerous pleomorphic vesicles that were round or oval and are generally larger than those seen in the mitral/tufted cells and are presynaptic to a symmetrical membrane thickening, a Gray Type 2 synapse. Mitral/tufted dendrites also tend to present with a more regular outline while periglomerular cell dendrites are irregular in outline and give rise to small appendages. In Figure 6D a mitral/tufted cell is making a dendrodendritic Gray Type 1 synapse onto a periglomerular cell dendrite while the reciprocal Gray Type 2 periglomerular cell to mitral/tufted cell dendrodendritic synapse is shown in Figure 6E. Although these were occasionally seen as reciprocal synaptic pairs within a single section, they were most often seen as single synapses as illustrated.

Figure 7: The frequency of axo- and dendrodendritic synapses per $40\mu m^2$ in the rat glomerulus. Abbreviations: MT, mitral or tufted cell dendrite; ORC, olfactory receptor cell axon; PG, periglomerular cell dendrite.

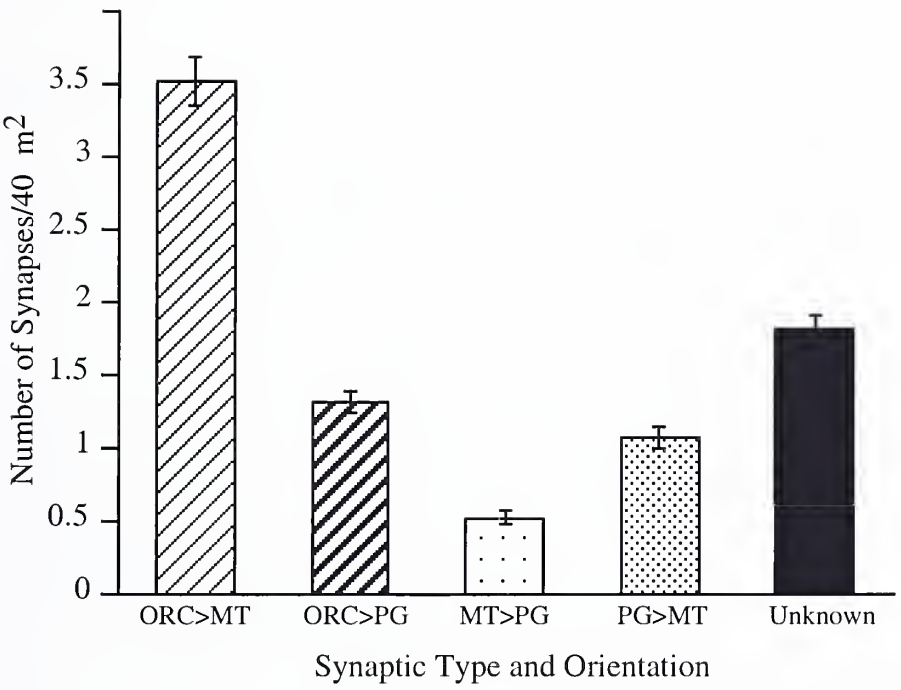
Number of Synapses/40 m2
3.5
3
2.5
2
1.5
1
0.5
0
ORC>MT
ORC>PG
MT>PG
PG>MT
Unknown
Synaptic Type and Orientation

The most abundant synapse category in the glomerulus was the olfactory nerve to mitral/tufted cell dendrite (3.51 +/- .17 synapses/40μm^2) followed by the olfactory nerve to periglomerular cell dendrite (1.31 +/- .08 synapses/40μm^2) (Figure 7). The dendrodendritic synapses found in the glomeruli did not correspond to the 1:1 ratio that has been previously reported. Mitral/tufted to periglomerular cell dendrites (0.52 +/- 0.05 synapses/40μm^2) occurred at less than half the frequency of the reciprocal periglomerular to mitral/tufted synapse (1.07 +/- .08 synapses/40μm^2) (Figure 7).

As we examined the distribution and morphology of synapses within the glomerulus the hypothesis emerged that the axodendritic and dendrodendritic synapses might be further segregated with respect to a single dendrite such that axodendritic synapses might be located on smaller and presumably more distal processes than the dendrodendritic synapses. To test this hypothesis we carried out measurements of the dendritic processes that were postsynaptic to ORC axons or periglomerular cells. The cross sectional diameters were significantly smaller in processes receiving axodendritic synapses than in those receiving dendrodendritic synapses from periglomerular cells. The diameter of mitral/tufted processes receiving dendrodendritic synapses (x= 1.53μm +/- 0.05) was significantly larger than the diameter of dendrites receiving afferent axodendritic synapses (x=0.82 μm +/- 0.03; $t=12.79$; $p<0.001$). This difference is apparent in Figure 6B where dendrites in a dendritic subcompartment (Den) can be contrasted with those in an axonal subcompartment (Ax). Note that there are many dendritic processes that have a relatively large diameter in the dendritic subcompartment whereas the individual dendrites in the axonal area (d) are smaller.

DEVELOPMENTAL

The olfactory bulb glomerulus is the site of the first synapse in the olfactory pathway. Axons from the olfactory receptor neurons in the olfactory epithelium terminate in the glomeruli on target dendrites from mitral, tufted and periglomerular neurons. It was recently established that the axons terminating in any one glomerulus are derived largely from olfactory receptor neurons that express the same odor receptor (Ressler et al., 1994; Vassar et al., 1994; Mombaerts et al., 1996). Thus each glomerulus in the olfactory bulb expresses a specific molecular phenotype based on the subset of receptor cells that innervate the glomerulus. These observations, coupled with prior functional analyses of the rat olfactory bulb (Stewart et al., 1979; Greer et al., 1982; Johnson et al., 1998, 1999), have provided strong support for the notion that the glomerulus is a fundamental organizational unit in odor coding (Shepherd, 1993). Similar conclusions have been reached based on both anatomical and functional analyses of glomeruli in several species including insects (e.g. Vickers et al., 1998) and crustaceans (e.g. Schmidt and Ache, 1992) (see Hildebrand and Shepherd, 1997 for review).

Initially, the glomerulus was viewed as a comparatively homogeneous structure in which primary afferent axons and target dendrites were uniformly distributed. However, more recent reconstructions of glomeruli have revealed a subcompartmental organization and segregation of synaptic circuits that was not previously recognized (Chao et al., 1997; Kosaka et al., 1997; Kasowski et al., 1999). In brief, the axons from olfactory receptor cells establish contiguous islands in the glomerulus within which they establish

synapses with isolated target dendrites. In contrast, the local circuit reciprocal dendrodendritic circuits are found within dendritic bundles that are segregated from the axonal islands by glial processes. The segregation of synapses appears significant for both the continual turnover of axons within glomeruli as well as the separation of primary afferent and local circuit synapses that are both using glutamate as their primary neurotransmitter.

Analyses of early development of the glomerulus have emphasized the seminal role of primary afferents in inducing the formation of glomeruli (Graziadei and Monti-Graziadei, 1986; Malun and Brunjes, 1996; Valverde et al., 1992; Treloar et al., 1999; Bailey et al., 1999). Glomeruli are first apparent in the mammal during late embryonic development and during the postnatal period increase in size and definition. There is now a general consensus that new glomeruli are not formed de novo beyond postnatal days 2-5 (Meisami and Sendera, 1993). However, functional analyses of olfactory bulb glomeruli using probes such as 2-deoxyglucose have suggested that mature, adult-like patterns of odor induced activity are not apparent until around the 2nd postnatal week (Greer et al., 1982). This suggests that while nascent glomeruli are present during the early postnatal period, substantive development/maturation continues for a more extended time. Support for this suggestion comes from the work of Hinds and Hinds (1976a,b) who demonstrated that synaptogenesis in the olfactory glomeruli of mice extended into the 2nd postnatal week. Similarly, Malun and Brunjes (1996) have shown that the elaboration of dendritic arbors in both the precoccial opossum and in the rat can extend well into the postnatal period.

To gain new insights into the maturation of glomeruli we have examined the expression of growth associated protein-43 (GAP-43) as a marker of immature olfactory receptor cell axons, olfactory marker protein (OMP) as a marker of mature olfactory receptor cell axons and synaptophysin as a marker of synaptic structure, in developing glomeruli. Our data demonstrate that the adult-like pattern of organization within glomeruli emerges around 12 days postnatal. In addition, the data strongly suggest that the topography of glomerular innervation by newly arriving axons changes as glomeruli mature. The results provide new insights into not only the mechanisms of glomerular development, but also some of the apparent prerequisites for adult-like functioning in glomeruli.

In general, the size of glomeruli increased proportionally to the age of the animal (Figure 8). As has been previously reported, while glomeruli can be detected during the perinatal period (Treloar et al., 1999), they are generally much smaller and more poorly defined by juxtaglomerular cells than at later ages (Greer et al., 1982; Meisami and Sendera, 1993; Malun and Brunjes, 1996).

OMP selectively stains olfactory receptor cell axonal processes and was used as a marker of mature axons while GAP-43 was employed to identify immature axons in the olfactory bulb (Verhaagen et a., 1989). The synaptic vesicle associated protein synaptophysin was utilized to distinguish synaptic specializations. At each of the ages tested the antibodies employed exhibited distinct laminar and sublaminar patterns of staining. There was no evidence to suggest that the epitopes recognized by each of the antibodies were changing over the course of development. The characteristics of the immunostaining are described below for each of the ages examined.

Figure 8: Light micrographs of cresyl violet stained sections of the rat olfactory bulb at postnatal days 0 (**A**), 6 (**B**), 12 (**C**) and 18 (**D**). At all ages glomeruli are readily identified as spherical areas of neuropil (e.g. asterisks) surrounded by the somata of juxtaglomerular cells. However, over the course of development the glomeruli increase in cross sectional diameter with a corresponding increase in the number of juxtaglomerular cells. ONL, olfactory nerve layer; GLL, glomerular layer; EPL, external plexiform layer; PND, postnatal day. Scale bar = 50 μm.

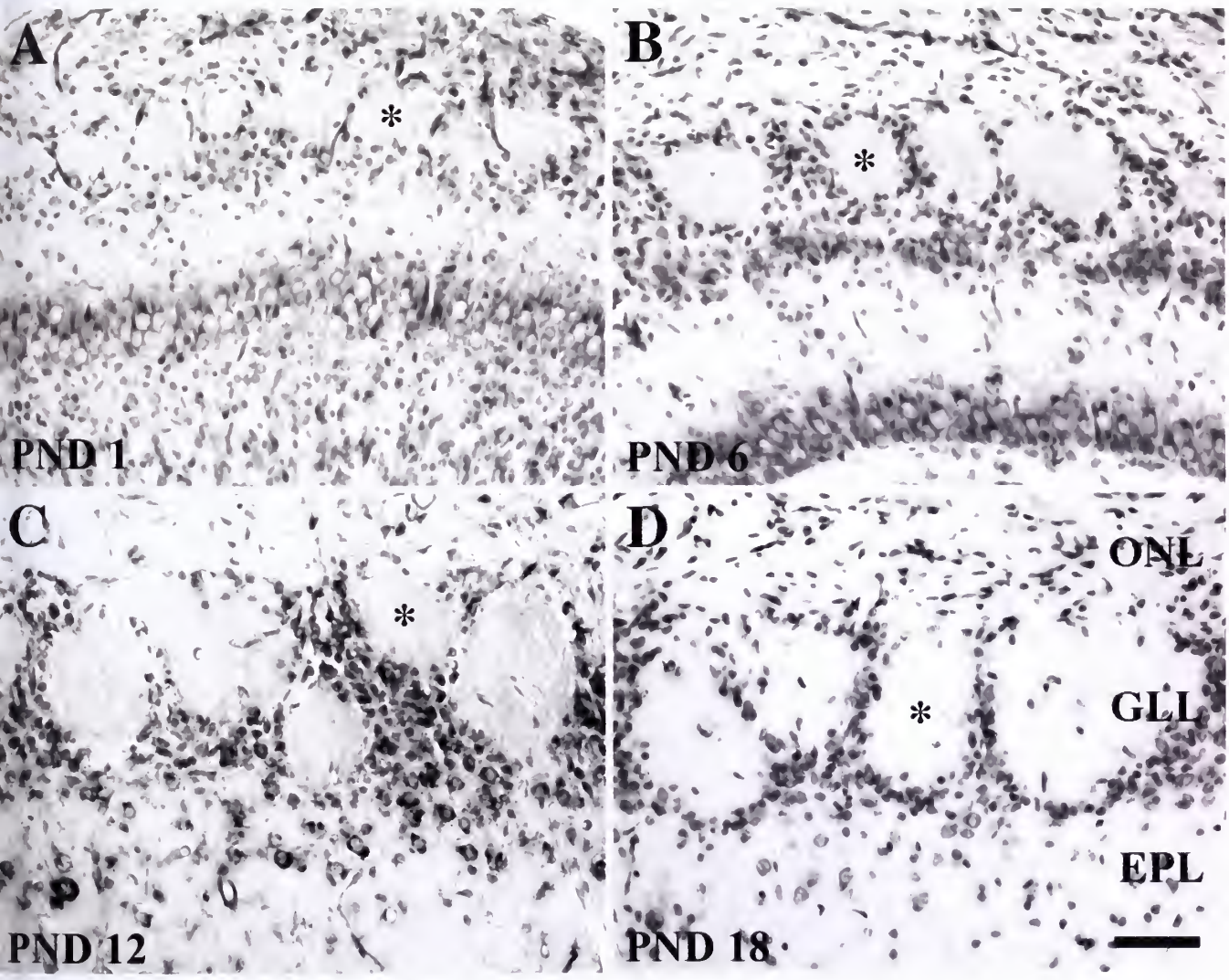
A
PND 1
B
PND 6
C
PND 12
D
ONL
GLL
EPL
PND 18

Figure 9: Confocal micrographs of olfactory marker protein (OMP), growth associated protein GAP-43, and synaptophysin immunoreactivity in the superficial layers of the rat olfactory bulb at postnatal day 1. **A,B**: OMP immunoreactivity in the olfactory nerve and glomerular layers appears diffuse and frayed. Axonal fascicles (e.g. arrow in B), travel through the nerve layer to target individual glomeruli. Within glomeruli areas of OMP immunoreactivity are interspersed with non-immunoreactive puncta (e.g. asterisk in B). In (A) an arrow indicates OMP^+ processes which extend beyond the inner boundaries of a glomerulus, toward the deeper regions of the olfactory bulb. **C,D**: GAP-43 staining is dense in the nerve layer while within glomeruli GAP-43 immunoreactivity often appeared more dense at the base of the many glomeruli, proximal to the nerve layer (e.g. arrow in C). **E,F**: Synaptophysin immunoreactivity clearly demarcates individual glomeruli. A punctate pattern of synaptophysin staining is evident within glomeruli. Varying levels of synaptophysin immunoreactivity as well as non-immunoreactive areas are also present. A similar distribution of synaptophysin staining is visible in the external plexiform layer (E). Non-immunoreactive processes within the glomerular and external plexiform layers likely correspond to blood vessels. ONL, olfactory nerve layer; GLL, glomerular layer; EPL, external plexiform layer; OMP, olfactory marker protein; GAP-43, growth associated protein-43; SYN, synaptophysin; PND, postnatal day. Scale bars = 25μm.

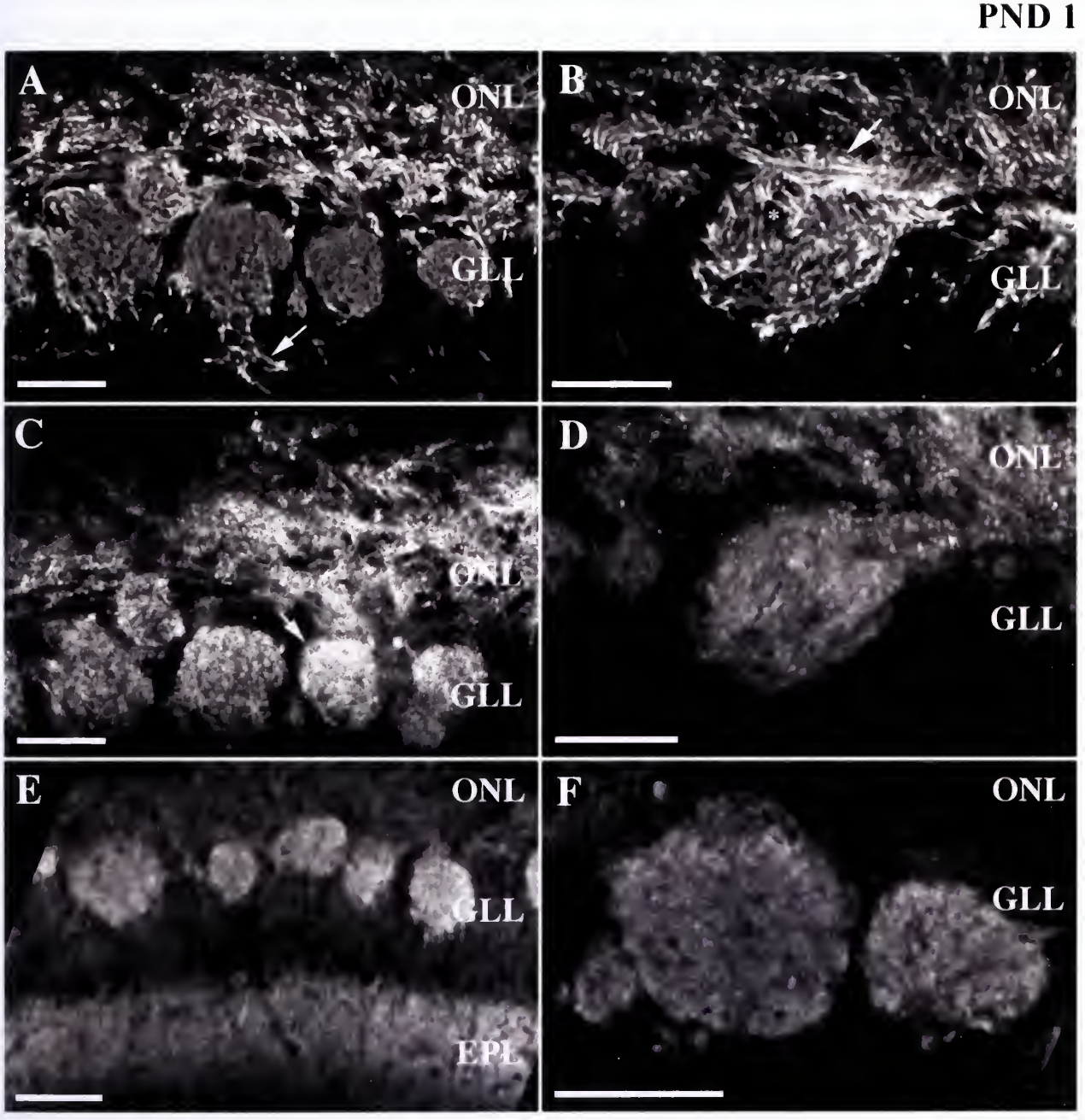
PND 1
A
ONL
GLL
B
ONL
GLL
OMP
C
ONL
GLL
D
ONL
GLL
GAP-43
E
ONL
GLL
EPL
F
ONL
GLL
SYN

Figure 10: Confocal micrograph of olfactory marker protein (OMP), growth associated protein GAP-43, and synaptophysin immunoreactivity in the superficial layers of the rat olfactory bulb at postnatal day 6. **A,B**: OMP staining is dense in the nerve layer where axonal fascicles (e.g. arrow in A) can be seen exiting the nerve layer to target a glomerulus. OMP immunoreactivity within glomeruli presents a more adult-like appearance. Discrete or single OMP^+ processes can be seen both exiting the nerve layer to indirectly enter a glomerulus (e.g. arrow in B) and extending from a glomerulus to travel distally towards the deeper layers of the olfactory bulb (e.g. arrowhead in B). **C,D**: GAP-43 immunoreactivity is generally diffuse and punctate, although some $GAP\text{-}43^+$ processes (e.g. arrow in C) can be identified. GAP-43 staining within glomeruli appears slightly more intense at the base, proximal to the nerve layer. **E,F**: Synaptophysin staining clearly demarcates glomeruli. Within glomeruli, a punctate pattern of synaptophysin immunoreactivity is interspersed with non-immunoreactive areas. A similar pattern of synaptophysin staining is apparent in the external plexiform layer. ONL, olfactory nerve layer; GLL, glomerular layer; EPL, external plexiform layer; OMP, olfactory marker protein; GAP-43, growth associated protein-43; SYN, synaptophysin; PND, postnatal day. Scale bars = 25μm.

PND 6

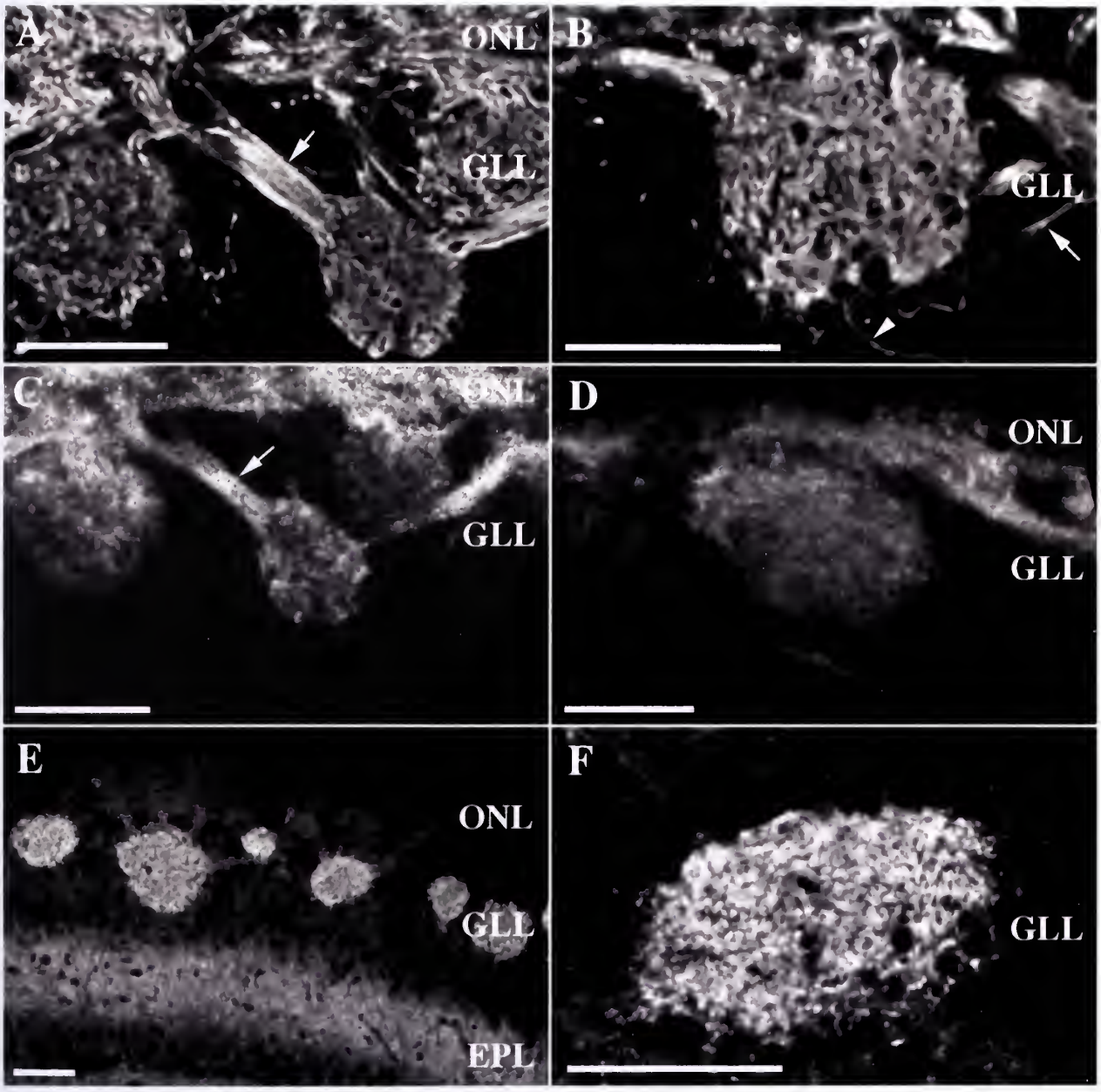

OMP

GAP-43

SYN

Figure 11: Confocal micrograph of olfactory marker protein (OMP), growth associated protein GAP-43, and synaptophysin immunoreactivity in the rat olfactory bulb at postnatal day 12. **A,B**: OMP immunoreactivity is dense in the nerve layer, where fascicles of axons (e.g. arrows in A and B), exit the nerve layer to enter glomeruli. Within glomeruli, contiguous islands of OMP staining (e.g. arrowhead in B), interdigitate with non-immunoreactive puncta (e.g. asterisks in B). **B,C**: The distribution of GAP-43 immunoreactivity appears more diffuse and granular than that of OMP. GAP-43 staining is dense in the nerve layer, where axonal fascicles (e.g. arrows in C) travel through the nerve layer to target a glomerulus. Within glomeruli, GAP-43^{+} processes (e.g. arrow in D) intersperse with non-immunoreactive areas (e.g. asterisks in D). GAP-43 immunoreactivity within glomeruli also appears slightly stronger at the apex, proximal to the nerve layer, and in the periphery of the glomerulus. **E,F**: Individual glomeruli are clearly demarcated by synaptophysin immunoreactivity. The distribution of synaptophysin staining is denser along the rim of the glomerulus (e.g. arrow in E). In (E) an arrowhead indicates an area of non-immunoreactivity within the external plexiform layer, where puncta of synaptophysin staining are otherwise broadly distributed throughout. These non-immunoreactive areas likely represent blood vessels cut within the plane of the tissue. ONL, olfactory nerve layer; GLL, glomerular layer; EPL, external plexiform layer; MCL, mitral cell layer; OMP, olfactory marker protein; GAP-43, growth associated protein-43; SYN, synaptophysin; PND, postnatal day. Scale bars = 25μm.

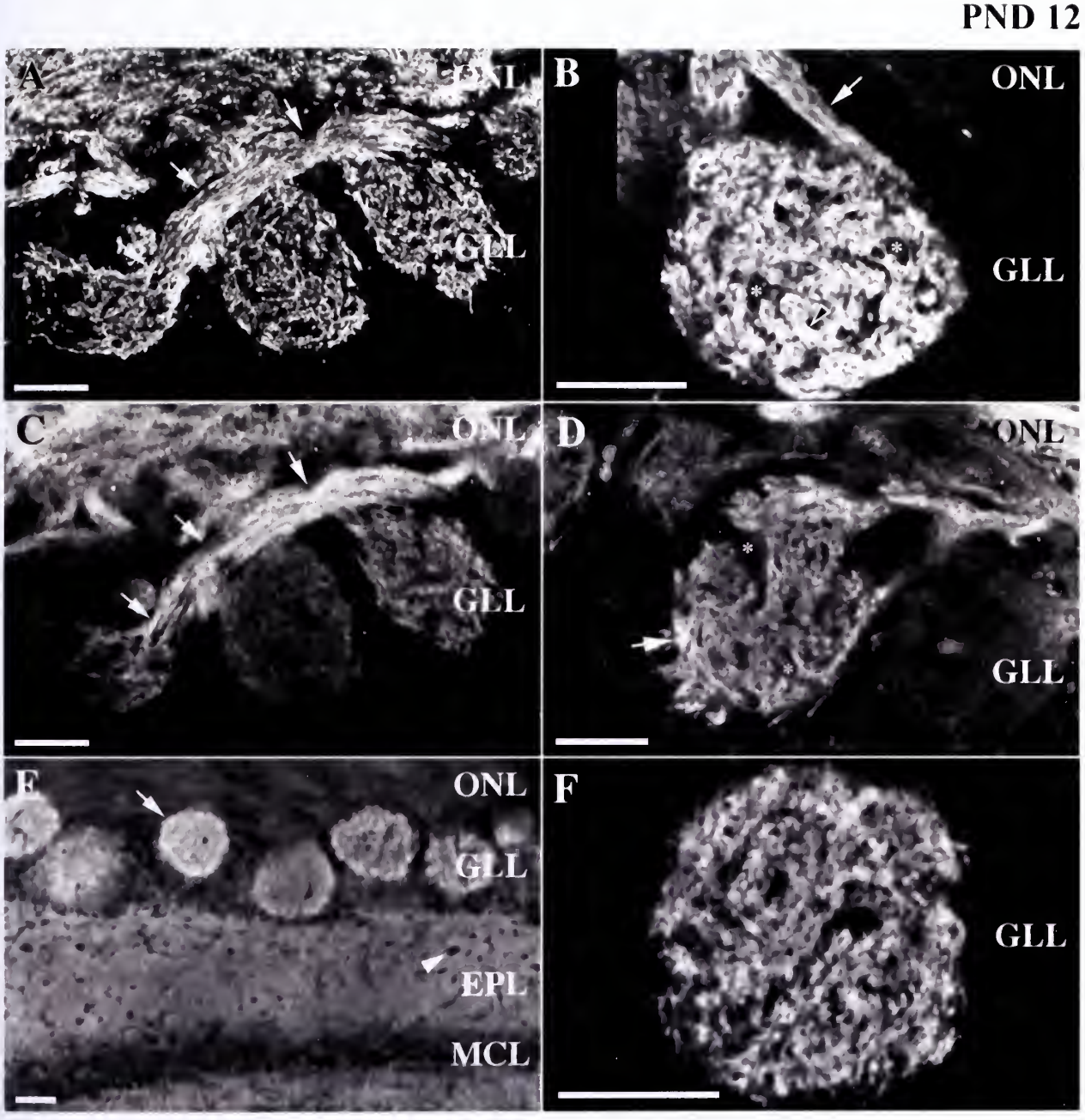
PND 12
A
ONL
GLL
B
ONL
GLL
OMP
C
ONL
GLL
D
ONL
GLL
GAP-43
E
ONL
GLL
EPL
MCL
SYN
F
GLL

Figure 12: Confocal micrograph of olfactory marker protein (OMP), growth associated protein GAP-43, and synaptophysin immunoreactivity in the rat olfactory bulb at postnatal day 18. **A,B**: OMP immunoreactivity appears similar to that at postnatal day 12, although the density of stained processes appears to have increased. As fascicles of axons (e.g. arrow in B) enter a glomerulus, OMP staining appears to diminish, which may reflect axon defasciculation. Within glomeruli, contiguous islands or zones of OMP staining interdigitate with discrete areas of non-immunoreactivity (e.g. asterisks in B). **C,D**: GAP-43 immunoreactivity appears generally more granular than OMP. Although GAP-43 staining appears variable throughout the glomerular layer, contiguous zones of GAP-43 immunoreactivity are evident within individual glomeruli. GAP-43 staining also exhibits a higher density at the apex, proximal to the nerve layer, and in the periphery of the glomerulus. **E,F**: A punctate pattern of synaptophysin staining is apparent in the glomerular and external plexiform layers. The distribution of synaptophysin staining does not exhibit the contiguous zones of staining seen with OMP; however, puncta lacking immunoreactivity (e.g. arrow in E) can be seen within glomeruli. These non-immunoreactive areas most likely correspond to blood vessels. ONL, olfactory nerve layer; GLL, glomerular layer; EPL, external plexiform layer; OMP, olfactory marker protein; GAP-43, growth associated protein-43; SYN, synaptophysin; PND, postnatal day. Scale bars = 25μm.

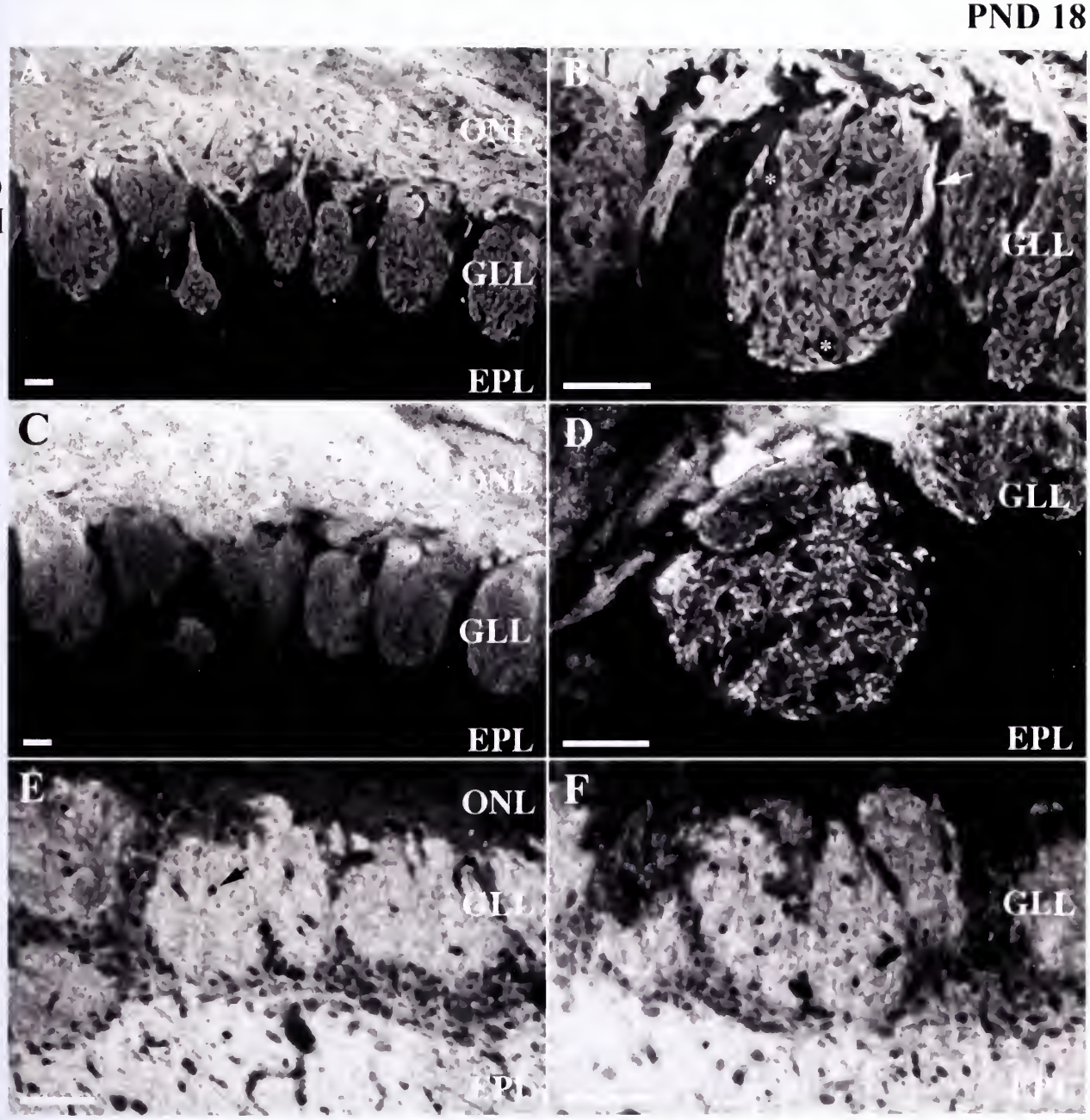
PND 18
OMP
GAP-43
SYN
A
ONL
GLL
EPL
B
GLL
C
GLL
EPL
D
GLL
EPL
E
ONL
GLL
F
GLL

Figure 13: Double labeled confocal images of olfactory marker protein (OMP), growth associated protein (GAP-43), and synaptophysin (SYN) immunoreactivity in the rat olfactory bulb at postnatal days 1 (A,B,C), 6 (D,E,F), 12 (G,H,I), and 18 (J,K,L). **A**: GAP-43 staining (red) is particularly prominent in the nerve layer with fewer OMP immunoreactive processes (green), evident at this age. Within glomeruli, OMP^+ processes (e.g. arrow) appear more distinct around the periphery, while $GAP\text{-}43^+$ processes appear to be distributed more densely within the core of the glomerulus. There is some evidence of colocalization (yellow) in the glomerular layer. **B**: OMP (green) is strongest in the nerve layer (e.g. arrow) with no evidence of synaptophysin immunoreactivity (red) or colocalization (yellow). Within glomeruli, however, colocalization is abundant. Areas of colocalization (e.g. arrowhead) interdigitate with puncta of OMP and synaptophysin staining as well as unstained areas throughout the glomerulus. **C**: GAP-43 only (red) is distinct in the nerve layer with no evidence of synaptophysin staining (green). Within the glomerular neuropil puncta of single labeling for synaptophysin and GAP-43 are evident, with some evidence of colocalization (yellow). **D**: Areas of OMP immunoreactivity (green), GAP-43 immunoreactivity (red), and colocalization or overlap (yellow) are evident in the nerve layer. Within glomeruli, GAP-43 staining and areas of colocalization with OMP are found in the central portions. However, in the circumferential regions of the glomerulus GAP-43 staining is largely absent while OMP staining is prominent. **E**: The nerve layer appears exclusively immunoreactive for OMP only (green). Colocalization with synaptophysin (yellow) is extensively distributed throughout the glomerular neuropil, where large areas of colocalization (e.g. arrowhead) interdigitate with puncta of OMP staining (e.g. arrow),

synaptophysin staining (e.g. double arrowheads), as well as unstained areas . **F**: GAP-43 immunoreactivity (red) is the predominate phenotype in the nerve layer. Within glomeruli GAP-43 staining is more evident in the central and more superficial, proximal to the nerve layer, regions of the glomerulus. Synaptophysin immunoreactivity (green) exhibits a punctate appearance within the glomerular neuropil, where little evidence of colocalization (yellow) with GAP-43 is seen. **G**: An arrow indicates a GAP-43$^+$ process (red) which is traveling through the nerve layer to target a glomerulus. The core of the glomerulus is occupied primarily by OMP$^+$ processes (green) (e.g. arrowhead), although puncta of GAP-43 staining (e.g. double arrowhead) can also be detected. In contrast with the pattern of staining seen at earlier ages, colocalization appears most distinct in the periphery or rim of the glomerulus. **H**: OMP immunoreactive processes (green), indicated by an arrow, are prominent in the nerve layer. Within glomeruli, colocalization of OMP and synaptophysin occurs extensively. Areas of colocalization appear to rest within islands of OMP staining, while punctate areas of synaptophysin staining (e.g. double arrowhead) are evident within glomeruli as well. **I**: Colocalization (yellow) of GAP-43 (red) and synaptophysin (green) staining is most distinct at the base, proximal to the nerve layer, and in the periphery of the glomerulus. Synaptophysin immunoreactivity, however, is more robust in the central region of the glomerulus, while GAP-43 immunoreactivity is more apparent in the periphery and superficial areas, proximal to the nerve layer. **J**: Areas of OMP immunoreactivity (green) (e.g. arrow), GAP-43 immunoreactivity (red), as well as colocalization or overlap (yellow), are evident within the nerve layer, reflecting various stages of axon maturity. Within glomeruli, GAP-43 staining (e.g. double arrowheads) is more apparent in the periphery of

the glomerulus, while OMP staining (e.g. arrowhead) remains more distinct in the core of the glomerulus. **K**: The nerve layer is predominately immunoreactive for OMP alone (green). The glomerular neuropil is largely occupied by extensive areas of OMP and synaptophysin colocalization (yellow) (e.g. arrow). These areas of colocalization within glomeruli are interspersed with discrete puncta of synaptophysin immunoreactivity (red) (e.g. double arrowhead) as well as OMP immunoreactivity (e.g. arrowhead). **L**: GAP-43 immunoreactivity is the predominate phenotype within the nerve layer, with little evidence of synaptophysin immunoreactivity (green) or colocalization (yellow). Colocalization within glomeruli is minimal compared with that seen in OMP and synaptophysin. GAP-43 staining is strongest in the periphery of the glomerulus, while synaptophysin staining is more robust in the core. ONL, olfactory nerve layer; GLL, glomerular layer; EPL, external plexiform layer; OMP, olfactory marker protein; GAP-43, growth associated protein-43; SYN, synaptophysin; PND, postnatal day. Scale bars = 25μm.

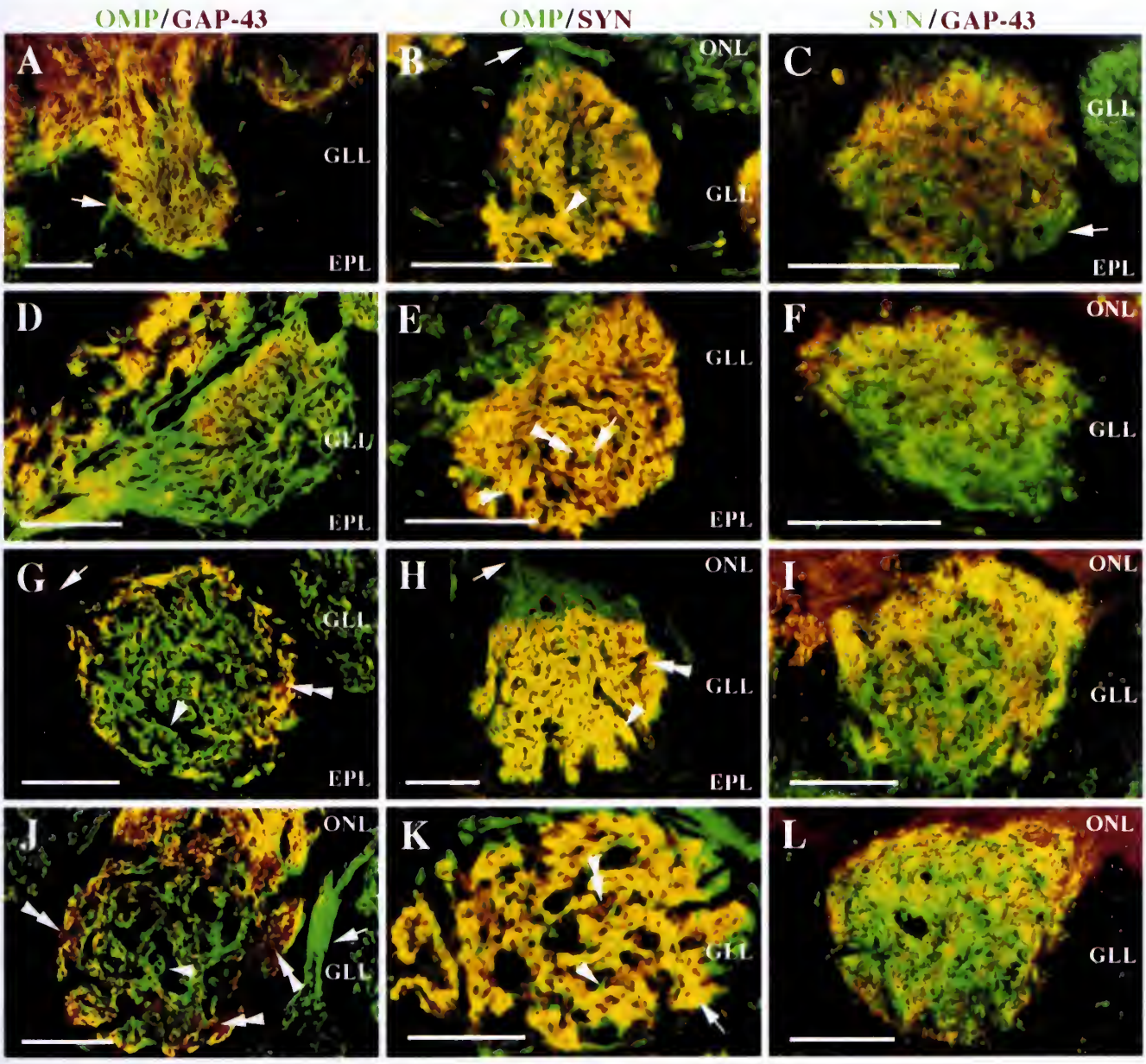
OMP/GAP-43
OMP/SYN
SYN/GAP-43
PND 1
PND 6
PND 12
PND 18
A
B
C
D
E
F
G
H
I
J
K
L
ONL
GLL
EPL

Postnatal Day 1

OMP

At postnatal day 1, OMP immunoreactive processes were evident in the olfactory nerve and glomerular layers (Figure 9A and B). In general, the immunoreactive processes in the nerve layer appeared relatively short and discontinuous, particularly in contrast to the patterns of staining described at older ages. The OMP^+ processes within the olfactory nerve layer did not appear as well-delineated axonal fascicles. Although in some cases the continuity with the glomerular layer could be detected (Figure 9B, arrow), it was less robust than seen at older ages. Rather, OMP^+ processes were broadly dispersed throughout the nerve layer in a seemingly disorderly arrangement. Similarly, OMP immunoreactivity within glomeruli demonstrated a frayed, diffuse appearance, and was interspersed with punctate areas of non-immunoreactivity distributed heterogeneously throughout each glomerulus (Figure 9B, asterisk). There were OMP^+ processes that appeared to extend beyond the inner boundaries of some glomeruli, towards the deeper regions of the olfactory bulb (Figure 9A, arrow).

GAP-43

GAP-43 immunoreactivity at postnatal day 1 demonstrated a more particulate quality as compared with the pattern of staining described below at older ages (Figure 9C and D). GAP-43 staining was dense in the olfactory nerve layer, although it was difficult to resolve single axons or discrete fascicles. The GAP-43 staining appeared punctate and did not reveal the longitudinal processes seen with OMP. Within glomeruli, GAP-43

immunoreactivity exhibited a diffuse and granular pattern of distribution which was interspersed with non-immunoreactive puncta throughout the glomerulus. In some glomeruli, GAP-43 staining exhibited a greater intensity proximal to the nerve layer (Figure 9C, arrow), while in others it appeared more evenly distributed. GAP-43 immunoreactivity was absent from both the juxtaglomerular zone and the external plexiform layer.

Synaptophysin

In general, synaptophysin immunoreactivity at postnatal day 1 (Figure 9E and F) was comparable to that seen at older ages. Synaptophysin staining was absent from the olfactory nerve layer. Individual glomeruli, however, were readily resolved due to the presence of synaptophysin^{+} elements. Individual processes could not be resolved with the synaptophysin staining. The intraglomerular synaptophysin staining appeared punctate with interdigitating areas of higher and lower immunoreactivity as well as zones within which no immunoreactivity was evident. Although synaptophysin immunoreactivity was absent from the periglomerular zone, the external plexiform layer showed a pattern of punctate synaptophysin staining interspersed with areas of non-immunoreactivity. The synaptophysin immunoreactivity seen in the external plexiform layer is most likely associated with the presynaptic dendrites while the non-immunoreactive areas likely correspond to blood vessels.

Double-Labeling

OMP/GAP-43 - Populations of GAP-43 immunoreactivity (shown in red) and OMP immunoreactivity (shown in green), as well as apparent areas of colocalization or overlap (shown in yellow) were present within the olfactory nerve layer (Figure 13A). However, at this age the predominant phenotype within the nerve layer was GAP-43$^+$. OMP$^+$ processes were evident as well, suggesting that some proportion of the axons at this age are exhibiting mature characteristics. While some co-localization of OMP and GAP-43 immunoreactivity is possible, these areas are more likely to represent axons (0.2 μm in diameter) overlapping within the 1 μm optical sections. In the glomeruli, both OMP$^+$ and GAP-43$^+$ processes were evident; however, OMP staining was slightly more apparent along the periphery and outermost portions of the glomerulus (Figure 13A, arrow), while GAP-43 staining appeared to remain within the more central areas of the glomerulus.

OMP/Synaptophysin - The olfactory nerve layer appeared to be almost exclusively immunoreactive for OMP (green) (Figure 13B, arrow), with no evidence of synaptophysin immunoreactivity (red) or colocalization (yellow) within the nerve layer (Figure 13B). In contrast, colocalization (Figure 13B, arrowhead) was abundant within glomeruli. However, interdigitating among the areas of colocalization were puncta that were only OMP or synaptophysin immunoreactive. Although immunoreactivity was not evident in the juxtaglomerular zone, the external plexiform layer demonstrated the punctate synaptophysin staining described above (no co-localization; not illustrated).

Synaptophysin/GAP-43- The olfactory nerve layer was strongly immunoreactive for GAP-43 but showed no evidence of labeling for synaptophysin (not illustrated; cf. Figure 9C and 9E). Within the glomerular neuropil punctate areas of synaptophysin

(green) and GAP-43 (red) immunoreactivity were evident (Figure 13C). However, the GAP-43 and synaptophysin showed comparatively little evidence of co-localization (yellow). The distribution of GAP-43 staining appeared slightly stronger proximal to the nerve layer and in the central portion of the glomerulus. In contrast, synaptophysin appeared more distinct in the circumferential region along the periphery of the glomerulus (Figure 13C, arrow). The juxtaglomerular zone did not show evidence of immunoreactivity. The external plexiform layer had no evidence of GAP-43$^+$ processes and therefore no examples of co-localization with the punctate synaptophysin immunoreactivity described above (not illustrated).

Postnatal Day 6

OMP

OMP staining in the olfactory nerve layer was very dense (Figure 10A and B). Fascicles as well as individual axons were seen traversing the nerve layer and targeting glomeruli (Figure 10A, arrow). Areas surrounding the fascicles devoid of OMP staining most likely represent the processes of ensheathing cells. OMP immunoreactivity within glomeruli was widely distributed, although less amorphous than that seen at postnatal day 1. In particular, the fibrous appearance seen at postnatal day 1 has been replaced with a more adult-like appearance, although the well delineated islands or zones of OMP immunoreactivity have not yet emerged. This pattern of OMP immunoreactivity appeared consistent throughout the glomerulus. Also visible were discrete bundles or single OMP positive processes that appeared to extend beyond the deeper boundaries of

the maturing glomerulus. Some of these OMP^+ processes appeared to emerge from the nerve layer to travel circuitously into a glomerulus (Figure 10B, arrow) and others appeared to protrude from a glomerulus to course distally, towards the external plexiform area (Figure 10B, arrowhead). OMP immunoreactivity was otherwise absent from the external plexiform layer as well as the periglomerular zone.

GAP-43

At postnatal day 6 (Figure 10C and D), the distribution of GAP-43 immunoreactivity exhibited a pattern which closely resembled that seen at postnatal day 1. In general, the staining exhibited a punctate appearance and was distributed in some cases along longitudinal processes. $GAP\text{-}43^+$ processes were abundant in the olfactory nerve layer, where fascicles of axons were seen targeting a glomerulus (Figure 10C, arrow). Within glomeruli, GAP-43 immunoreactivity appeared slightly more intense proximal to the nerve layer. Of note, the overall distribution of staining within glomeruli did not appear as zones of immunoreactivity interspersed with punctate areas of non-immunoreactivity as observed at the older ages described below, but instead demonstrated a more diffuse pattern of staining reminiscent of that seen at postnatal day 1. The periglomerular zone and external plexiform layer were devoid of immunoreactivity.

Synaptophysin

As was noted for postnatal day 1, synaptophysin staining clearly demarcated the glomeruli, in part due to the absence of staining in the olfactory nerve layer and

periglomerular zone (Figure 10E and F). Within the glomerular layer however, staining was dense throughout the length of each glomerulus. A punctate pattern of synaptophysin immunoreactivity interspersed with areas of non-immunoreactivity was seen within glomeruli. Although what appeared to be single fibers could be followed, the overall impression was one of highly intense puncta throughout the glomerulus. Although the juxtaglomerular zone showed little immunoreactivity, the external plexiform layer demonstrated a punctate pattern of staining. Scattered areas of non-immunoreactivity likely represent blood vessels.

Double Labeling

OMP/GAP-43 - Areas of OMP immunoreactivity (green), GAP-43 immunoreactivity (red), and co-localization (yellow) were evident within the olfactory nerve layer (Figure 13D). There appeared to be some heterogeneity however, since in some regions of the olfactory bulb OMP staining appeared more abundant than GAP-43 while elsewhere in the olfactory bulb, OMP and GAP-43 staining appeared more evenly distributed (not illustrated). Within glomeruli, both OMP and GAP-43 immunoreactivity demonstrated patterns resembling those described above for each of the markers. Little or no co-localization was seen within the glomerular layer. In the periglomerular zone and external plexiform layer, we observed no evidence of OMP or GAP-43 immunoreactivity.

OMP/Synaptophysin - The olfactory nerve layer appeared to be immunoreactive for OMP only (green) with little, if any, evidence of synaptophysin (red), and no evidence of colocalization (yellow), as was noted previously at postnatal day 1 (Figure

13E). Within glomeruli, however, large areas of colocalization were apparent throughout the neruopil. Puncta of co-localization often appeared superimposed on areas of OMP only staining, giving the appearance of yellow/red dots on a green background. In addition, areas with no immunoreactivity and puncta of single labeling for synaptophysin (Figure 13E, double arrowhead) and OMP alone (Figure 13E, arrow) appeared to interdigitate with areas of co-localization (Figure 13E, arrowhead) within the glomerulus. This pattern of staining was consistent throughout the glomerulus. The juxtaglomerular zone was devoid of staining; however, the external plexiform layer exhibited the complex distribution of synaptophysin immunoreactivity described for postnatal day 1 (not illustrated).

GAP-43/Synaptophysin - In the olfactory nerve layer, although GAP-43 immunoreactivity (red) was evident, no indication of co-localization was found since synaptophysin staining was not present in the nerve layer (see above) (Figure 13F). Within glomeruli the distribution of synaptophysin staining had a diffuse punctate appearance, as described above. Similarly, GAP-43 staining within glomeruli in these double label preparations was as described above. Co-localization of synaptophysin and GAP-43 was minimal in the glomerular neuropil. In those regions that did exhibit evidence of co-localization, it was most prominent in the portion of the glomerulus proximal to the nerve layer. While the periglomerular area was devoid of staining, the external plexiform layer showed the complex pattern of synaptophysin immunoreactivity described above, with no evidence of GAP-43 staining (not illustrated).

Postnatal Day 12

OMP

At postnatal day 12, the distribution of OMP immunoreactivity appeared similar to that previously described in the adult (Kasowski et al., 1999). Staining was very dense in the olfactory nerve layer, where fascicles of axons coursed longitudinally and were seen exiting the nerve layer to enter olfactory bulb glomeruli (Figure 11A and B, arrows). Within the nerve layer, and particularly in fascicles targeting specific glomeruli (Figure 11B, arrow), elongated areas lacking immunoreactivity were seen interdigitating with the OMP immunoreactive processes. As noted above, these most likely represent the ensheathing cell processes that surround olfactory receptor cell axon fascicles. Within the glomeruli, contiguous islands of OMP immunoreactivity (Figure 11B, arrowhead) were interspersed with non-immunoreactive puncta (Figure 11B, asterisks). These were first seen at postnatal day 6, but became more distinctive by postnatal day 12. Staining for OMP was not apparent in the juxtaglomerular zone or in the external plexiform layer.

GAP-43

The distribution of GAP-43 immunoreactivity was generally similar to that of OMP, although the appearance of immunoreactivity for GAP-43 was generally more granular and diffuse (Figure 11C and D). Staining was dense in the olfactory nerve layer, where axonal fascicles could be seen running parallel to the nerve layer and passing into glomeruli (Figure 11C, arrows). Within glomeruli, GAP-43 immunoreactivity (Figure 11D, arrow) interspersed with discrete areas that were not immunoreactive (Figure 11D, asterisks). The islands of GAP-43 immunoreactivity, however, appeared less well

delineated that those seen with OMP, and the areas of staining within the islands had a more diffuse appearance (cf. Figure 11A and 11C). GAP-43 immunoreactivity was not uniformly distributed throughout a glomerulus but appeared to exhibit a slightly greater intensity proximal to the nerve layer and along the outer rim and circumference of the glomerulus. There was no evidence of GAP-43 specific staining in the juxtaglomerular areas or in the external plexiform layer.

Synaptophysin

As we noted above for the younger animals, the olfactory nerve layer was generally devoid of synaptophysin immunoreactivity. Individual glomeruli, however, were readily demarcated by synaptophysin immunoreactivity (Figure 11E and F). In general, the synaptophysin staining was more diffuse than that seen with either OMP or GAP-43; synaptophysin staining was not restricted to the discrete zones or islands of contiguous staining seen with OMP and GAP-43. The punctate distribution of synaptophysin staining was not homogeneous throughout a glomerulus, rather staining appeared more dense around the periphery or rim of the glomerulus (Figure 11E, arrow). In the external plexiform layer a similarly distinct pattern of staining was evident (Figure 11E). Although synaptophysin immunoreactivity was densely distributed throughout the external plexiform layer, puncta of non-immunoreactivity were broadly spread throughout (Figure 11E, arrowhead). These areas of non-immunoreactivity broadly distributed in glomeruli and the external plexiform layer most likely represent, at least in part, blood vessels cut both longitudinally as well as transversely within the plane of the tissue.

Double Labeling

OMP/GAP-43 - The occurrence of double labeling with markers for OMP and GAP-43 were comparable to the patterns described for each of the markers alone (Figure 13G). The olfactory nerve layer exhibited immunoreactivity for OMP alone, GAP-43 alone (Figure 13G, arrow), as well as areas of colocalization (not illustrated). The latter most likely reflects the superpositioning of the olfactory receptor cell axons, although it may be that in some cases both epitopes could occur within single axons during maturation. Throughout the olfactory nerve layer, these populations of immunoreactivity appeared in various combinations and densities, although all three phenotypes were generally present (not illustrated). The distribution of OMP^+ and $GAP\text{-}43^+$ processes within the glomerular neuropil appears fundamentally different from that seen at earlier ages. The core of the glomerulus appears immunoreactive predominately for OMP (green) (Figure 13G, arrowhead) although a few scattered $GAP\text{-}43^+$ (red) (Figure 13G, double arrowhead) processes can be detected. The region in which GAP-43 and OMP appear to overlap the most, however, is the periphery or rim of the glomerulus. This is in contrast with the pattern seen at younger ages in which the core of the glomerulus was predominately $GAP\text{-}43^+$ while the more mature OMP^+ processes were found in the periphery of the glomerulus. Both the juxtaglomerular zone and external plexiform area appeared to be devoid of immunoreactivity.

OMP/Synaptophysin - Co-localization of OMP and synaptophysin occurred extensively within the glomerular neuropil (Figure 13H). These areas of colocalization appeared to rest within the islands of OMP immunoreactivity described above (Figure

13H, arrowhead). However, other areas within these islands showed immunoreactivity for OMP alone, while punctate processes immunoreactive for synaptophysin alone were found within the glomerulus as well (Figure 13H, double arrowhead). There was an absence of immunoreactivity in the juxtaglomerular zones, but the external plexiform layer exhibited the distinct pattern of synaptophysin immunoreactivity described above for the younger ages.

GAP-43/Synaptophysin - Colocalization of GAP-43 and synaptophysin was evident throughout the glomerulus, but was predominate proximal to the nerve layer and in the periphery, as was the distribution of GAP-43 immunoreactivity within the glomerulus (Figure 13I). Synaptophysin immunoreactivity, however, was more robust in the central region of the glomerulus.

Postnatal Day 18

OMP

At postnatal day 18, OMP immunoreactivity was equivalent to that described for postnatal day 12, although it does appear that the density or number of stained processes may have increased (Figure 12A and B). Fascicles of axons were seen traveling both parallel and perpendicular to the layers of the olfactory bulb (Figure 12A). Within the olfactory nerve unstained areas appear as well. These may reflect the presence of immature axons (see GAP-43 below) or the ensheathing cell glia that contribute to the formation of axon fascicles. As the fascicles entered glomeruli the immunoreactivity appeared to diminish slightly, perhaps due to the defasciculation of the axons (Figure

12B, arrow). Within the glomeruli, the OMP immunoreactivity appeared broadly distributed within contiguous zones or islands that interdigitate with non-immunoreactive puncta of varying sizes (Figure 12B, asterisks). As we have previously shown, the latter most likely correspond to the dendritic and glial processes found within the glomeruli as well as transversely and longitudinally cut blood vessels (Kasowski et al., 1999). In general, OMP immunoreactivity was qualitatively uniform across the population of olfactory bulb glomeruli. The juxtaglomerular zones were devoid of OMP immunoreactivity, as were the deeper layers of the olfactory bulb.

GAP-43

GAP-43 immunoreactivity (Figure 12C and D) had a distribution at postnatal day 18 somewhat comparable to that of OMP. Staining was dense in the olfactory nerve layer where complexes of fascicles, as described above for OMP, were seen. As the fascicles enter glomeruli the immunoreactivity appeared to diminish significantly. Within the glomeruli, GAP-43 staining appeared similar to OMP in that contiguous subglomerular zones appeared more heavily stained, though they lack the sharp delineation seen with the OMP staining. Moreover, GAP-43 immunoreactivity was not consistent throughout the glomerulus, but appeared to exhibit a higher density proximal to the nerve layer and in the peripheral, circumferential regions of the glomerulus. In contrast to OMP, GAP-43 immunoreactivity appeared variable across the population of glomeruli (Figure 12C, cf. Figure 13J). Although slight staining within juxtaglomerular areas was occasionally observed, it tended to be less than that seen in the nerve layer or glomeruli.

Synaptophysin

Synaptophysin immunoreactivity was not found in the olfactory nerve layer (Figure 12E and F). In the glomerular layer, however, a dense reaction product was present throughout the glomeruli. The individual zones, seen so clearly with OMP, were absent although several puncta lacking immunoreactivity were found within the glomeruli (Figure 12E, arrow). These unstained puncta most likely correspond to blood vessels. The juxtaglomerular zone lacked any specific immunoreactivity for synaptophysin immunoreactivity but the deeper external plexiform layer exhibited a complex pattern of non-immunoreactive puncta broadly distributed within an otherwise intense area of synaptophysin immunoreactivity.

Double-Labeling

OMP/GAP-43 - Similar populations of immunoreactivity were seen in double-labeled images using markers for OMP and GAP-43: OMP only (green), GAP-43 only (red), and areas of colocalization/overlap (yellow) (Figure 13J). In the nerve layer, colocalization of OMP and GAP-43 is most likely due to the superpositioning of axons. Areas of superpositioning of $GAP\text{-}43^{+}$ and OMP^{+} processes in the nerve layer were interspersed throughout with single labeling for OMP (Figure 13J, arrow) and GAP-43, whose distributions appeared heterogeneous across different regions of the nerve layer. These differences in OMP and GAP-43 immunoreactivity at different regions in the bulb may reflect general variations in axon maturity in any given area within the nerve layer. Colocalization in the glomerulus remained dense proximal to the nerve layer and appeared to decrease as fascicles enter the glomeruli. Within glomeruli, staining for both

OMP and GAP-43 was apparent throughout the glomerulus, although OMP immunoreactivity (Figure 13J, arrowhead) appeared more concentrated in the center/core of the glomerulus while GAP-43 (Figure 13J, double arrowheads) appeared more concentrated in the periphery of the glomerulus. This was consistent with observations made of single labeling, described above as well as the pattern that had begun to emerge at postnatal day 12. The juxtaglomerular zone and external plexiform area appeared devoid of immunoreactivity (not illustrated).

OMP/Synaptophysin - Three populations of immunoreactivity were evident in sections double-labeled with markers for OMP and synaptophysin: OMP staining alone (green), synaptophysin alone (red), and regions of colocalization (shown in yellow) (Figure 13K). The nerve layer expressed OMP alone; there was no evidence of synaptophysin in the nerve layer. Within glomeruli, however, large areas of colocalization were found throughout a glomerulus (Figure 13K, arrow). These regions of colocalization were punctate in appearance and resided within the islands of OMP-positive processes. Areas of colocalization were interspersed with discrete puncta of OMP (Figure 13K, arrowhead) and synaptophysin (Figure 13K, double arrowhead) immunoreactivity, and the density of colocalization seemed consistent throughout a glomerulus. The juxtaglomerular zone lacked any immunoreactivity, but the external plexiform layer showed the complex pattern of synaptophysin staining described for earlier ages, and appeared to be devoid of both OMP-positive processes and colocalization (not illustrated).

GAP-43/Synaptophysin - The distribution of double labeling for GAP-43 (red) and synaptophysin (green) was consistent with the patterns described above for the two

markers alone at postnatal day 18 (Figure 13L). GAP-43 immunoreactive processes were evident in the nerve layer, from which synaptophysin appeared to be entirely absent. Colocalization was evident within glomeruli, although markedly less than that seen with synaptophysin and OMP. Staining for synaptophysin alone was strongest in the core of the glomerulus while staining for GAP-43 alone appeared strongest in the periphery of the glomerulus. As noted previously, staining was absent from the juxtaglomerular zone, and no evidence of co-localization of these epitopes was found in the external plexiform layer.

Discussion

The findings from the first study examining subcompartmental organization within olfactory bulb glomeruli in the adult will be discussed first, followed by those from the second study investigating subcompartmental organization during postnatal development.

The major finding emerging from the first study is that the mammalian glomerulus is not a homogenous unit but can be divided into subcompartments which differ in their cellular and synaptic organization. The data contributing to this conclusion can be summarized as follows: 1) Within a glomerulus there are interdigitating subcompartments that are composed predominantly of either axons or dendrites. 2) Each subcompartment is further characterized by its synaptic connections. Primary afferent axodendritic synapses are found exclusively in axonal zones while dendrodendritic local circuit synapses are found primarily in dendritic subcompartments. 3) Analysis of the glomerular distribution of synaptic vesicle associated proteins was consistent with the suggestion that primary afferent and local synaptic circuits are segregated into subglomerular compartments.

Characterization of Axonal and Dendritic Subcompartments

Immunocytochemical analyses of OMP revealed the compartmental nature of subglomerular organization. Axonal areas, identified by dense OMP-IR, are found adjacent to areas devoid of OMP-IR. Double labeling for OMP and MAP2 demonstrated

that dendritic processes arborized predominately within the non-OMP areas thus revealing an interdigitating pattern of OMP-IR and MAP2-IR zones.

EM reconstructions of glomeruli further demonstrated the segregation of axonal and dendritic compartments. Axonal areas tended to form semi-contiguous zones of electron dense processes that interdigitated with the electron lucent dendrites. Within the axonal areas single or small groups of dendritic processes, most likely from mitral/tufted and periglomerular cells, were diffusely distributed throughout the axonal zone. In contrast, dendritic areas were composed exclusively of dendrites without evidence of any axonal processes. Moreover, dendritic zones were often encapsulated, at least in part, by glial processes which segregated the dendritic and axonal compartments. The dendritic compartments included bundles of from 4-100+ dendrites. This contrasts with dendritic bundles previously described in cortex where only 10-20 dendrites traveled in closely apposed clusters (Roney et al., 1979). Moreover, no evidence of dendrodendritic synapses has been reported for cortical dendritic bundles. Dendritic versus axonal compartments were readily recognized at the ultrastructural level. While, as noted above, there was a continuum of size, the exclusion of ORC axons from the dendritic zone was a reliable index, as were the distribution of synapses (vide infra).

Synaptic Characterization of the Glomerulus

It has been generally held that intraglomerular synaptic organization is homogeneous (Pinching and Powell, 1971). However, our data reveal a segregation of primary afferent and local circuit synapses. Primary afferent axodendritic synapses were found where individual or small groups of dendrites penetrated into axonal

subcompartments and to a lesser extent along the interface between the axonal and dendritic subcompartments. Axodendritic synapses were not found within the dendritic compartments. In contrast, dendrodendritic synapses occurred predominately in dendritic subcompartments and were only rarely observed between dendrites in axonal subcompartments.

The immunocytochemical analyses also suggested a heterogeneous distribution of synapses. Synaptophysin colocalized strongly with primary afferent axons in the axonal subcompartments while synapsin 1 appeared strongly associated with dendrites in the dendritic subcompartments. Earlier studies suggested that vesicle associated proteins may segregate across olfactory bulb synapses because synaptophysin and synapsin 2 were heaviest in the glomeruli while synaptoporin and synapsin 1 were heaviest in the external plexiform layer (Bergmann et al., 1993; Stone et al., 1994). Because the current study demonstrates that primary afferent synapses occur in the axonal compartment of the glomerulus while the dendrodendritic synapses occur in the dendritic compartment, it seems reasonable to suggest that synaptophysin is most strongly associated with the axodendritic synapse while synapsin 1 is most strongly associated with the dendrodendritic synapse. A differential synaptic localization of vesicle associated proteins has also been found previously in the retina (Mandell et al., 1990) and hippocampus (Zürmohle et al., 1994).

While the specific mechanism that may underlie a differential distribution of vesicle associated proteins in the olfactory bulb is not yet known, it is provocative to note that the synaptology of the primary afferent and local circuit synapses of the olfactory bulb are distinct with regard to their collections of vesicles (Price, 1968). Primary

afferent synapses are characterized by a large collection of small spherical vesicles and a thick asymmetrical postsynaptic thickening. The dendrodendritic synapse from mitral/tufted to periglomerular dendrites is similarly organized but usually includes only a few (2-10) vesicles in the presynaptic compartment. The reciprocal dendrodendritic synapses from the periglomerular cell dendrite includes a larger collection of pleomorphic vesicles and a symmetrical postsynaptic thickening. Such differences seem likely to contribute to the differential distribution of vesicle associated proteins.

We did not quantify the synaptic connections of the centrifugal axons which project in small numbers into the glomerulus (Shipley and Ennis, 1996) and most likely contribute, in part, to the unknown synapses in Figure 7. Chao et al. (1997), however, suggested that centrifugal axons may occur in the dendritic compartments of the glomerulus and indeed, have previously noted that choline acetyltransferase containing centrifugal axons appeared to be restricted from areas within glomeruli that contained high numbers of primary afferent axons (Kasa et al., 1995). Because centrifugal axons are, by definition, modulatory in nature, it seems plausible that they would terminate proximal to local circuit dendrodendritic synapses in the dendritic compartments of glomeruli. However, in the absence of a centrifugal-specific marker, it would have been difficult in our analyses to establish the frequency or distribution of this relatively small population of axons (Le Jeune and Jourdan, 1993; Kasa et al., 1995).

The diameters of dendritic processes receiving axodendritic synapses were significantly smaller than those receiving dendrodendritic synapses. This suggests a laminar segregation of synapses with respect to the glomerular dendritic arbor of mitral and tufted cells. The thicker, more proximal portions of the dendritic shaft may be

clustered with other dendrites in the dendritic subcompartments and participate in dendrodendritic synapses. The finer, more distal, processes might then penetrate into the axonal subcompartments to receive axodendritic synapses. Such an organization would maximize inhibitory local circuit regulation of the ORC input to dendrites and further, would be consistent with the segregation of excitatory and inhibitory synapses onto cortical neurons (i.e. Beaulieu and Collonier, 1985). Finally, the separation of axodendritic and dendrodendritic synapses appears to be a prudent organizational scheme for the glomerulus, in part, because both the ORC axons and the mitral cells use glutamate as a neurotransmitter (Berkowicz et al., 1994; Ennis et al., 1996; Trombley and Shepherd, 1993). Segregation of the synaptic circuits may thus be important in order to minimize non-specific effects due to the diffusion of neurotransmitter.

The quantitative distribution of axo- and dendrodendritic synapses in the glomerulus was consistent with prior reports in that the former was more frequent than the latter (Hinds and Hinds, 1976; White, 1973). Unexpectedly, however, symmetrical periglomerular to mitral/tufted cell synapses occurred at a ratio of 2:1 relative to the reciprocal mitral/tufted to periglomerular synapses. White (1973) previously reported that mitral/tufted to periglomerular and the reciprocal periglomerular to mitral/tufted dendrodendritic synapses occurred in roughly equal numbers, although a breakdown of frequency was not reported. More consistent with our current findings, Hinds and Hinds (1976) reported that the mitral/tufted to granule and/or periglomerular dendrodendritic synapse was predominant by a ratio of 2.8:1 through postnatal day 44 in mice. These data suggest that the ratios of the glomerular dendrodendritic circuits may differ somewhat from those more fully characterized in the external plexiform layer of the

Figure 14: Summary model of the possible organization in the mammalian glomerulus. Axon fascicles 1 and 2 enter the glomerulus, defasciculate and distribute into smaller axonal subcompartments which interdigitate with dendritic subcompartments. Within the axonal subcompartments the axons make primary afferent synapses with isolated or small groups of dendrites from mitral, tufted and periglomerular cells. Dendrodendritic synapses are rarely seen in the axonal areas. Dendritic subcompartments contain bundles of dendrites that are encompassed by glial processes (thick gray line). In dendritic subcompartments, dendrites are closely apposed and establish dendrodendritic synaptic circuits. Axodendritic synapses were not seen in the dendritic compartments. Thus, primary afferent axodendritic and local circuit dendrodendritic synapses are separated within the glomerulus. The insets illustrate the types of synaptic specializations found within the axonal and dendritic subcompartments of the glomerulus. Axodendritic synapses are characterized by a high density of uniform spherical synaptic vesicles and are presynaptic to an asymmetrical membrane thickening on mitral/tufted and periglomerular cells. Mitral/tufted cells have uniform small, round vesicles that are presynaptic to an asymmetrical membrane thickening, a Gray Type 1 synapse. The periglomerular cells have more numerous pleomorphic vesicles that are round or oval and are generally larger than those seen in the mitral/tufted cells. The periglomerular dendrites are presynaptic to a symmetrical membrane thickening, a Gray Type 2 synapse. Abbreviations: AF, axon fascicle; Axon term., olfactory receptor cell axon terminal; Den, dendritic subcompartment; PG, periglomerular cell; MT, mitral or tufted cell.

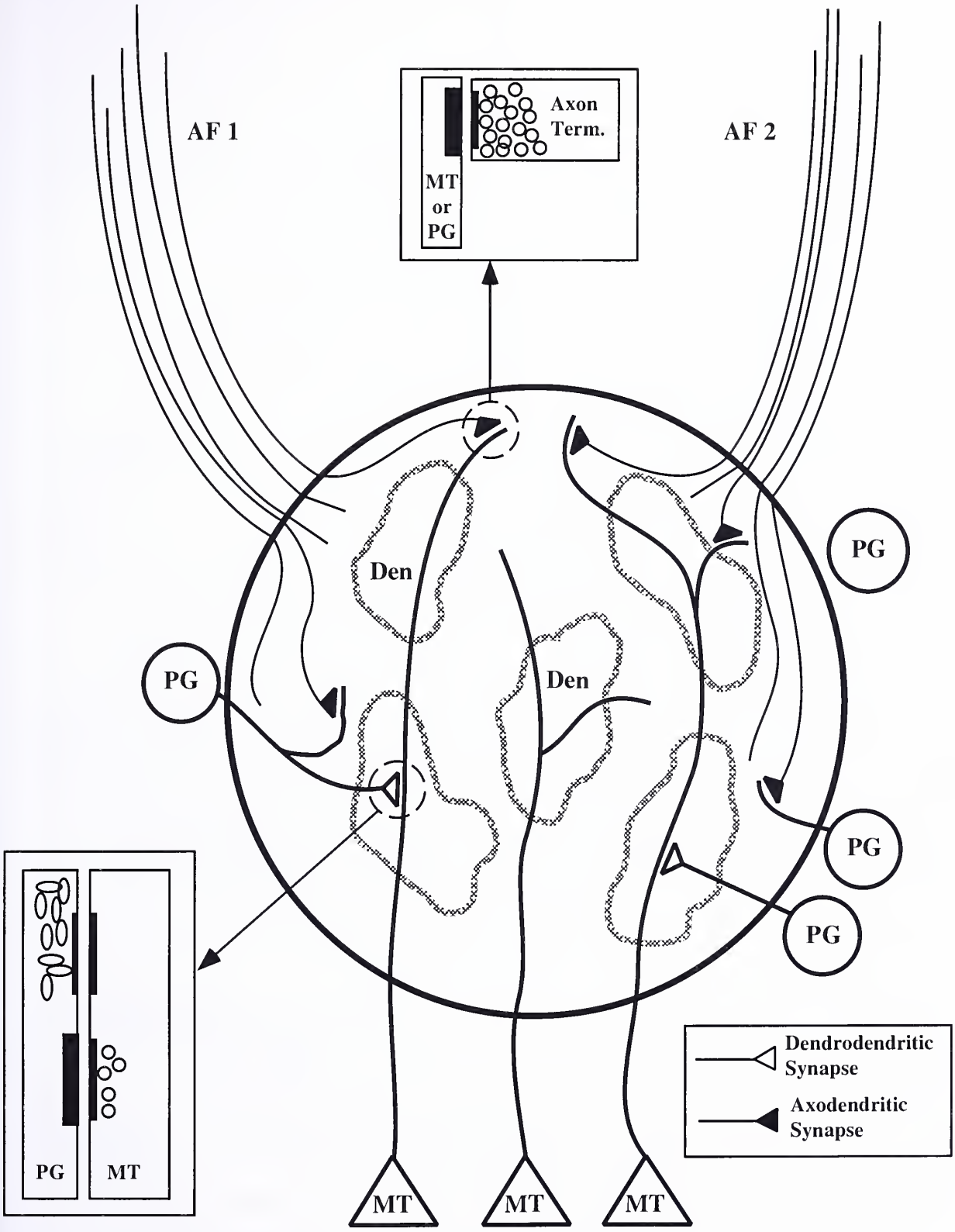
AF 1
AF 2
Axon
Term.
MT
or
PG
Den
Den
PG
PG
PG
PG
MT
MT
MT
PG
MT
Dendrodendritic
Synapse
Axodendritic
Synapse

olfactory bulb (Price and Powell, 1970) and that further analyses of serially sectioned glomerular dendrites would be appropriate.

Hinds (1970) reported the presence of synaptic triads in the olfactory bulb glomerulus. Axodendritic synapses onto dendrites that were also engaged in reciprocal/serial dendrodendritic synapses were apparent in single electron micrographs. White (1973) similarly suggested the presence of such triads, although no examples were provided. Clear evidence for these complex serial synaptic arrangements was not seen in the current study. However, among the rare dendrodendritic synapses occurring within the axonal zones, as well as those axodendritic synapses found at the interface of the axonal and dendritic compartments, there is clearly the potential for such synaptic arrangements to occur. However, our analysis of the data suggest that while a single dendrite could be involved in serial and/or reciprocal synaptic circuits, each of the synapses is likely to be separated from each other and would not appear in the side-by-side arrangement characteristic of the dendrodendritic synapses in the external plexiform layer (Price and Powell, 1970; Greer and Hálasz, 1987.)

Model and Functional Implications

Based on our interpretation of the data, organization in the mammalian glomerulus may be summarized as shown in Figure 14. As ORC axons enter the glomerulus they defasciculate, arborize and distribute in large contiguous zones. Within the axonal zones the most terminal portions of dendritic processes receive axodendritic synapses from the ORC axons. Dendritic processes exhibit a far more complex distribution. A single dendrite, upon entering the glomerulus, may pass through both

axonal and dendritic compartments. The dendritic compartment, containing 4-100 tightly apposed dendrites, is demarcated from the axonal compartment, in part, by a surrounding glia process. In addition, the dendritic compartment is distinguished by the presence of numerous dendrodendritic synapses. While dendrodendritic synapses were seen in the axonal zone, they were rare. Axodendritic synapses were not observed with dendritic zones. Thus, while a dendrite can pass through both zones and receive both axo- and dendrodendritic synapses, the spatial distribution of those synapses is defined by the subglomerular compartment.

It has been recognized for some time that glomeruli in insects and crustaceans can be regionally subdivided based on cytological and neurochemical differences. Schmidt and Ache (1992) showed that cap/subcap regions of glomeruli are morphologically distinct and innervated by different classes of interneurons in the antennal lobe of the spiny lobster. Recently they also identified additional intraglomerular layers using immunoreactivity to antibodies against several neurotransmitters (Schmidt and Ache, 1997). Such regionalization has been similarly demonstrated in the moth, *Manduca sexta*, and in the cockroach, *Periplaneta americana* (Boeckh and Tolbert, 1993; Hansson et al., 1991).

The heterogeneity found in insects and lobsters was not thought to be present in single vertebrate glomeruli until recently. Kosaka et al. (1997) and Toida et al. (1998) identified subgroups of immunoreactive processes in the glomerulus in the rat and suggested prominent differences in the distribution of periglomerular cell dendrites and ORC axons within glomeruli. Chao et al. (1997) also recognized a heterogeneous organization of glial cells within single glomeruli. They observed that glial cells were

restricted to dendritic compartments and were excluded from a separate compartment which contained primarily ORC axons. Consistent with our findings, the glial cells were seen to form a partial border between compartments. Our findings extend these previous studies by showing: 1) that clusters of dendrites and contiguous fields of ORC terminals establish well defined subcompartments within the glomerulus; and, 2) that synaptic vesicle associated proteins and categories of synapses are differentially distributed in the dendritic and ORC terminal compartments within single glomeruli. Collectively, these data support the hypothesis that information processing is regionally subdivided within the mammalian glomerulus.

The most important findings to emerge from the second study include: 1) The emergence of a mature or adult-like subcompartmental organization within the glomerulus by 12 days postnatal; 2) a temporal-spatial pattern of axonal maturation within the glomerulus with the most immature axons initially found in the core while later in development, they occupy more peripheral regions; 3) The strong colocalization of OMP and synaptophysin in contrast with less frequent colocalization of synaptophysin and GAP-43. Each of these findings will be discussed, in turn, below.

GAP-43 and OMP proved to be effective markers of immature and mature, respectively, olfactory receptor cell axons. Although GAP-43 is a membrane constituent and OMP a cytoplasmic protein, because olfactory receptor cell axons average 0.2μm in diameter and because we used 1.0μm optical images to assess the data, this difference in subcellular localization seems unlikely to have biased the data. Similarly, although the

presence of GAP-43 in other processes including juxtaglomerular cells and centrifugal axons had the potential to influence our interpretation of the data, this seems unlikely for the following reasons. First, the majority of GAP-43 staining in the developing glomerular layer occurs within the glomerular neuropil (cf. Figs. 9-12) where growing olfactory receptor cell axons continue to arrive. There was little evidence of GAP-43 staining in the juxtaglomerular zone in either the current or previous reports (Treloar et al., 1999; Bailey et al., 1999; Verhaagen et al., 1989). Second, expression by either developing centrifugal axons or juxtaglomerular processes is transient and diminish as they mature over a relatively narrow timeframe (Bayer, 1983). Thus, while we cannot rule out that some GAP-43 staining not associated with olfactory receptor cell axons would be found in the early postnatal period, it seems unlikely that it would confound our interpretation of the data.

Subcompartmental Organization of the Glomerulus

Prior studies established that the adult glomerulus exhibits a complex subcompartmental organization in which the axodendritic synapses made by olfactory receptor cell axons and the local circuit dendrodendritic synapses made by efferent dendrites are spatially segregated within the glomerulus (Chao et al., 1997; Kasowski et al., 1999). At the earliest ages tested in this study, 1 and 6 days postnatal, there was no evidence of a differential distribution of olfactory receptor cell axons within the glomerulus. Rather OMP^+ and $GAP\text{-}43^+$ processes appeared homogeneously distributed throughout the glomerulus. The initial appearance of an adult-like pattern of distinct islands of OMP^+ processes was at 12 days postnatal with further refinement of immunoreactive and non-immunoreactive zones by 18 days postnatal. These results are

consistent with the results of Malun and Brunjes (1996) who showed that prior to 10 days postnatal, the glomerular arbors of mitral cell apical dendrites exhibited variable degrees of differentiation. Indeed, at postnatal day 4 examples of mitral cells with multiple apical dendrites and sparsely developed glomerular tufts were illustrated (Malun and Brunjes, 1996). These observations suggest the possibility that the subcompartmental organization of the glomerulus emerges as the dendritic arbors mature and segregate into the dendritic bundles that then interdigitate among the islands of olfactory receptor cell axons within the glomerulus. Also consistent with this interpretation are the developmental studies of Hinds and Hinds (1976a,b) who showed that axodendritic synaptic circuits emerge initially in the glomerulus with a later appearance and maturation of dendrodendritic circuits. Indeed, the frequency of axodendritic synapses in the perinatal period exceeds that of dendrodendritic synapses by at least an order of magnitude. Consequently, it seems reasonable to suggest that the synaptophysin staining we observed at postnatal days 1 and 6 is most likely accounted for largely by the terminals of olfactory receptor cell axons. However, as the animals mature, the density or frequency of both axodendritic and dendrodendritic synapses within the glomerulus asymptotes around 10 – 12 days postnatal in the mouse. This appears consistent with the maturation of glomerular organization around 12 days postnatal. The colocalization of OMP and synaptohphysin staining interdigitating with smaller islands of synaptophysin alone staining is indicative of the segregation of the axo- and dendrodendritic circuits into separate compartments. Finally, this pattern of maturation is reminiscent of that reported by Oland et al. (1990) in the moth; initially protoglomeruli in the antennal lobe

reflect largely the distribution of primary afferent axons, the target dendritic processes do not organize into glomerular structures until around midstage 6.

Maturation of functional measures in the olfactory bulb follows a timecourse similar to that reported here. Using 2-deoxyglucose, both Greer et al. (1982) as well as Astic and Saucier (1982) reported that while individual glomeruli could be detected following odor stimulation at younger ages, the definitive patterns characteristic the adult did not appear until around postnatal day 12. Similarly, Meisami and Sendera (1993) using cytochrome oxidase staining, reported increases in both the number and size of glomeruli that appear to correspond well to the data reported here. Glomeruli more than doubled in diameter between postnatal days 1 and 25 while the total number of glomeruli in the bulb had stabilized by 3 days postnatal. Our data now suggest that while glomeruli may continue to increase in diameter, most likely due to the addition of new primary afferents as well as juxtaglomerular dendrites, the compartmental organization is established by 12 days. Further growth of individual glomeruli after 12 days postnatal most likely reflects the elaboration of the established adult pattern.

Maturation Within the Glomerular Neuropil

Little is known about the spatio-temporal sequences of maturation within a glomerulus. Our prior studies of the embryonic rat olfactory bulb demonstrated that immature axons arrived first in the core of a glomerulus and were then displaced to the periphery during ensuing maturation (Treloar et al., 1999). Our current data demonstrate that this pattern of development continues through postnatal day 6. However, by postnatal day 12 the pattern inverts; the immature fibers, visualized as GAP-43^{+} processes, now define the outermost periphery of the glomerulus. It is notable that this

pattern of maturation is also reflected in the synaptophysin staining which tends to appear heaviest in the periphery of the glomerulus. A similar pattern of synaptophysin staining is also noted in the adult (Stone et al., 1994; Johnson et al., 1996). These data suggest that the initial formation of the glomerulus is likely to incorporate a scheme in which the most immature axons move toward the periphery as they mature, and the glomerulus grows. However, when a glomerulus becomes adult-like or mature, axons appear to enter only after coursing around the periphery of the glomerulus. This may lead, in the adult, to an initially heavier concentration of both mature and immature axons in the periphery of the glomerulus. Some support for this suggestion may be found in Johnson et al. (1996) who reported that concentrations of synaptophysin immunoreactivity were heaviest in glomeruli where they were proximal to the olfactory nerve layer. In a related context, Halasz and Greer (1993) and Klenoff and Greer (1998) both presented evidence of accumulations of axons in the periphery of glomeruli. Verhaagen et al. (1989) also reported heavy accumulations of GAP-43 immunoreactivity around the perimeter of glomeruli in the adult. Similarly, Holtmaat et al. (1997) showed that following over-expression of GAP-43, olfactory receptor cell axons distributed preferentially in the periphery of the glomerulus. The mechanism that may mediate this change in the approach of axons to glomeruli in adults versus neonates remains to be established. However, it may reflect alterations in the distribution and the molecular properties of the astroglia cells that both surround and invade the neuropil of glomeruli (Chiu and Greer, 1996; Bailey and Shipley, 1993; Gonzalez et al., 1993; Kasowski et al., 1999).

Synaptophysin Localization

There is a general consensus that olfactory receptor cell axons lose the GAP-43 phenotype as they mature and begin to express OMP (Verhaagen et al., 1989). We previously reported that in the embryo synaptophysin was lightly expressed in olfactory nerve when it abuts the presumptive olfactory bulb at embryonic day 17, prior to a robust expression of OMP (Treloar et al., 1999). The current data are consistent in that they too suggest only slight co-localization of synaptophysin and GAP-43. Rather, synaptophysin appears most consistently co-localized with OMP expression. This simple observation is consistent with the notion that OMP expression is associated with more mature axons that have established synaptic appositions within the glomeruli. Interestingly, at the youngest ages we examined it was difficult to dissociate the OMP and synaptophysin co-localization. It was not until postnatal day 12 that a more adult like pattern emerged in which puncta of synaptophysin staining alone interdigitated with the islands of co-localized OMP and synaptophysin. Johnson et al. (1996) present similar findings in that their synaptophysin staining of glomeruli was more homogeneous at perinatal ages than in older animals. As has been shown in the adult, synaptophysin localization is not limited to the axodendritic synapses in the olfactory bulb; synaptophysin immunoreactivity is also found in the glomerular reciprocal dendrodendritic synapses (Kasowski et al., 1999; Stone et al., 1994). Consequently, the most plausible explanation for the findings in the current study is the emergence of the nascent dendritic bundles and their dendrodendritic synaptic circuits.

Summary

In conclusion, the data presented demonstrate that the compartmental organization of olfactory receptor cell axons within glomeruli emerges slowly over the first 12 postnatal days. Compartmentalization appears to increase in concert with the upregulation of the OMP phenotype and downregulation of the GAP-43 phenotype. The appearance of puncta of synaptophysin staining, interdigitating with islands in which OMP and synaptophysin colocalized, heralded the emergence of the dendritic bundles within the glomeruli.

References

Astic, L. and D. Saucier (1982) Ontogenesis of the functional activity of rat olfactory bulb: autoradiographic study with the 2-deoxyglucose method. Developmental Brain Research *2*:243-256.

Bähler M, Benfenati F, Valtorta F, Greengard P (1990) The synapsins and the regulation of synaptic function. Bioessays *126*: 259-263.

Bailey M.S., A.C. Puche, M.T. Shipley (1999) Development of the olfactory bulb: evidence for glia-neuron interactions in glomerular formation. The Journal of Comparative Neurolology 415:423-48

Bailey, M.S. and M.T. Shipley (1993) Astrocyte subtypes in the rat olfactory bulb: morphological heterogeneity and differential laminar distribution. The Journal of Comparative Neurology *328*:501-526.

Baker, H., M. Grillo, and F.L. Margolis (1989) Biochemical and immunocytochemical characterization of olfactory marker protein in the rodent central nervous system. The Journal of Comparative Neurology *285*:246-261.

Bayer, S.A. (1983) ^{3}H-thymidine-radiographic studies of neurogenesis in the rat olfactory bulb. Experimental Brain Research *50*:329-340.

Beaulieu, C., and M. Collonier (1985) A laminar analysis of the number of round-asymmetrical and flat symmetrical synapses on the spines, dendrite trunks, cell bodies in area 17 of the cat. J. Comp. Neurol. *231:*180-189.

Bergmann, M., T. Schuster, D. Grabs, B. Marqueze-Pouey, H. Betz, H. Traurig, A. Mayerhofer, and M. Gratzl (1993) Synaptophysin and synaptoporin expression in the developing rat olfactory system. Dev. Brain Res. *74*: 235-244.

Berkowicz, D.A., P.Q. Trombley, and G.M. Shepherd (1994) Evidence for glutamate as the olfactory receptor cell neurotransmitter. J. of Neurophysiol. *71*: 2557-2561.

Boeckh, J. and L.P. Tolbert (1993) Synaptic organization and development of the antennal lobe in insects. Microscopy Res. Tech. *24*: 260-280.

Buonviso, N. and M.A. Chaput (1990) Response similarity to odors in olfactory bulb output cells presumed to be connected to the same glomerulus: electrophysiological study using simultaneous single-unit recordings. J. Neurophysiol. *63*:447-454.

Caceres, A., G. Banker, and L. Binder (1986) Immunocytochemical localization of tubulin and microtubule-associated protein 2 during development of hippocampal neurons in culture. J. Neurosci. *6*: 714-722.

Chao, T.I., P. Kasa, and J.R. Wolff (1997) Distribution of astroglia in glomeruli of the rat main olfactory bulb:exclusion from the sensory subcompartment of neuropil. The Journal of Comparative Neurology *388*:191-210.

Chiu, K. and C.A. Greer (1996) Immunocytochemical analyses of astrocyte development in the olfactory bulb. Developmental Brain Research *95*:28-37.

Doucette, R. (1993) Glial cells in the nerve fiber layer of the main olfactory bulb of embryonic and adult mammals. Microscopy Res. Tech. *24*: 113-130.

Ennis, M., L.A. Zimmer, and M.T. Shipley (1996) Olfactory nerve stimulation activates rat mitral cells via NMDA and non-NMDA receptors in vitro. NeuroReport *7*: 989-992.

Gong, Q. and M.T. Shipley (1995) Evidence that pioneer olfactory axons regulate telencephalon cell cycle kinetics to induce the formation of the olfactory bulb. Neuron *14*:91-101.

Gonzalez, M.L., C.J. Malemud, and J. Silver (1993) Role of astroglial extracellular matrix in the formation of rat olfactory bulb glomeruli. Experimental Neurology *123*:91-105.

Graziadei, P.P.C. and G.A. Monti-Graziadei (1986) Principles of organization of the vertebrate olfactory glomerulus: an hypothesis. Neuroscience *19*:1025-1035.

Greer, C.A. and N. Hálasz (1987) Plasticity of dendrodendritic microcircuits following mitral cell loss in the olfactory bulb of the murine mutant Purkinje cell degeneration. The Journal of Comparative Neurology *256*:284-298.

Greer, C.A., W.B. Stewart, M.H. Teicher, and G.M. Shepherd (1982) Functional development of the olfactory bulb and a unique glomerular complex in the neonatal rat. The Journal of Neuroscience *2*:1744-1759.

Guthrie, K.M. and C.M. Gall (1995) Odors increase Fos in olfactory bulb neurons including dopaminergic cells. NeuroReport *6*: 2145-2149.

Halasz, N. and C.A. Greer (1993) Terminal arborizations of olfactory nerve fibers in the glomeruli of the olfactory bulb. The Journal of Comparative Neurology *337*:307-316.

Hansson, B.S., T.A. Christensen, and J.G. Hildebrand (1991) Functionally distinct subdivisions of the macroglomerular complex in the antennal lobe of the male sphinx moth Manduca sexta. J. Comp. Neurol. *312*: 264-278.

Hildebrand, J.G. and G.M. Shepherd (1997) Mechanisms of olfactory discrimination: converging evidence for common principles across phyla. Annual Review of Neuroscience *20*: 595-632.

Hinds, J.W. (1970) Reciprocal and serial dendrodendritic synapses in the glomerular layer of the rat olfactory bulb. Brain Research *17*:530-534.

Hinds, J.W. and P.L. Hinds (1976a) Synapse formation in the mouse olfactory bulb: quantitative studies. The Journal of Comparative Neurology *169*:15-40.

Hinds, J.W. and P.L. Hinds (1976b) Synapse formation in the mouse olfactory bulb. II. Morphogenesis. The Journal of Comparative Neurology *169*:41-61.

Holtmaat, A.J.G.D., W.T.J.M.C. Hermens, M.A.F. Sonnemans, R.J. Giger, F.W. Van Leeuwen, M.G. Kaplitt, A.B. Oestreicher, W.H. Gispen, and J. Verhaagen (1997) Adenoviral vector-mediated expression of B-50/GAP-43 induces alterations in the membrane organization of olfactory axon terminals in vivo. The Journal of Neuroscience *17*:6575-6586.

Jahn R., T.C. Sudhof (1994) Synaptic vesicles and exocytosis. Annual Review of Neuroscience17:219-46.

Jahn, R., W. Schiebler, C. Quimet, and P. Greengard (1985) A 38,000-dalton membrane protein (p38) present in synaptic vesicles. Proc. Natl. Acad. Sci. U.S.A. *82*: 4137-4141.

Jastreboff, P.J., P.E. Pedersen, C.A. Greer, W.B. Stewart, J.S. Kauer, T.E. Benson, and G.M. Shepherd (1984) Specific olfactory receptor populations projecting to identified glomeruli in the rat olfactory bulb. Proceedings of the National Academy of Sciences,USA *81*:5250-5254.

Johnson, B.A., C.C. Woo, and M. Leon (1998) Spatial coding of odorant features in the glomerular layer of the rat olfactory bulb. The Journal of Comparative Neurology *393*:457-471.

Johnson, B.A., C.C. Woo, K. Ninomiya-Tsuboi, and M. Leon (1996) Synaptophysin-like immunoreactivity in the rat olfactory bulb during postnatal development and after restricted experience. Developmental Brain Research *92*:24-30.

Jourdan, F., Duveau, A., Astic. L., and A. Holley (1980) Spatial distribution of [14C] 2-deoxyglucose uptake in the olfactory bulbs of rats stimulated with two different odours. Brain Res. *188(1):*139-54.

Kasa, P., I. Hlavati, E. Dobo, A. Wolff, F. Joó, and J.R. Wolff (1995) Synaptic and non-synaptic cholinergic innervation of the various types of neurons in the main olfactory bulb of adult rat: Immunocytochemistry of choline acetyltransferase. Neurosci. *67*:667-677.

Kasowski, H.J., H. Kim, and C.A. Greer (1999) Compartmental organization of the olfactory bulb glomerulus. The Journal of Comparative Neurology *407*:261-274.

Klenoff, J.R. and C.A. Greer (1998) Postnatal development of olfactory receptor cell axonal arbors. The Journal of Comparative Neurology *390*:256-267.

Kosaka, K., K. Toida, F.L. Margolis, and T. Kosaka (1997) Chemically defined neuron groups and their subpopulations in the glomerular layer of the rat main olfactory bulb-II. prominent differences in the intraglomerular dendritic arborization and their relationship to olfactory nerve terminals. Neuroscience *76*:775-786.

Kosaka, K., K. Toida, Y. Aika, and T. Kosaka (1998) How simple is the organization of the olfactory glomerulus?: the heterogeneity of so-called periglomerular cells. Neuroscience Research *30*:101-110.

Kosaka, K., Y. Aika, K. Toida, C.W. Heizmann, W. Hunziker, D.M. Jacobowitz, I. Nagatsu, P. Streit, T.J. Visser, and T. Kosaka (1995) Chemically defined neuron groups and their subpopulations in the glomerular layer of the rat main olfactory bulb. Neurosci. Res. *23*:73-88.

Lancet, D., C.A. Greer, J.S. Kauer, and G.M. Shepherd (1982) Mapping of odor-related neuronal activity in the olfactory bulb by high-resolution 2-deoxyglucose autoradiography Proc. Natl. Acad. Sci. U.S.A. *79*: 670-674.

Le Jeune, H., and F. Jourdan (1993) Cholinergic innervation of olfactory glomeruli in the rat: an ultrastructural immunocytochemical study. J. Comp. Neurol. *336(2):*279-92.

Malun, D. and P.C. Brunjes (1996) Development of olfactory glomeruli: temporal and spatial interactions between olfactory receptor axons and mitral cells in opossums and rats. The Journal of Comparative Neurology *368*:1-16.

Mandell, J.W., A.J. Czernik, P. DeCamilli, P. Greengard, and E. Townes-Anderson (1992) Differential expression of synapsins I and II among rat retinal synapses. J. Neurosci. *12*: 1736-1749.

Mandell, J.W., E. Townes-Anderson, A.J. Czernik, R. Cameron, P. Greengard, and P. DeCamilli (1990) Synapsins in the vertebrate retina: absence from ribbon synapses and heterogeneous distribution among conventional synapses. Neuron *5*: 19-33.

Margolis, F.L. (1972) A brain protein unique to the olfactory bulb Proc. Natl. Acad. Sci. U.S.A. *69*: 1221-1224.

Margolis, F.L. (1985) Olfactory marker protein: from PAGE band to cDNA clone. Trends in Neurosciences *8*:542-546.

Meiri K.F., M. Willard , M.I. Johnson (1988) Distribution and phosphorylation of the growth-associated protein GAP-43 in regenerating sympathetic neurons in culture. The Journal of Neuroscience 8:2571-2581.

Meisami, E. and T.J. Sendera (1993) Morphometry of rat olfactory bulbs stained for cytochrome oxidase reveals that the entire population of glomeruli forms early in the neonatal period. Developmental Brain Research *71*:253-257.

Mombaerts, P. (1996) Targeting olfaction. Current Opinion in Neurobiology *6*:481-486.

Mombaerts, P., F. Wang, C. Dulac, S.K. Chao, A. Nemes, M. Mendelsohn, J. Edmondson, and R. Axel (1996) Visualizing an olfactory sensory map. Cell *87*: 675-686.

Monti-Graziadei, G.A., R.S. Stanley, and P.P.C. Graziadei (1980) The olfactory marker protein in the olfactory system of the mouse during development. Neuroscience *5*:1239-1252.

Mori, K., K. Kishi, and H. Ojima (1983) Distribution of dendrites of mitral, displaced mitral, tufted, and granule cells in the rabbit olfactory bulb. J. Comp. Neurol. *219*: 339-355.

Mori, K., N. Mataga, and K. Imamura (1992) Differential specificities of single mitral cells in rabbit olfactory bulb for a homologous series of fatty acid odor molecules. J. Neurophysiol. *67*: 329-355.

Oland, L.A., G. Orr, and L.P. Tolbert (1990) Construction of a protoglomerular template by olfactory axons initiates the formation of olfactory glomeruli in the insect brain. The Journal of Neuroscience *10*:2096-2112.

Onoda, N. (1992) Odor-induced fos-like immunoreactivity in the rat olfactory bulb. Neurosci. Lett. *137*:157-160.

Orona, E., E.C. Rainer, and J.W. Scott (1984) Dendritic and axonal organization of mitral and tufted cells in the rat olfactory bulb. J. Comp. Neurol. *226*: 346-356.

Philpot, BD., JH. Lim, S. Halpain, and PC Brunjes (1997) Experience-dependent modifications in MAP2 phosphorylation in rat olfactory bulb. J. Neurosci. *17(24)*:9596-604.

Pinching, A.J. and T.P.S. Powell (1971) The neuropil of the glomeruli of the olfactory bulb. J. Cell Sci. *9*: 347-377.

Price, J.L. (1968) The synaptic vesicles of the reciprocal synapse of the olfactory bulb. Brain Research *11*:697-700.

Price, J.L. and T.P.S. Powell (1970) The synaptology of the granule cells of the olfactory bulb. Journal of Cell Science *7*:125-155.

Ressler, K.J., S.L. Sullivan, and L.B. Buck (1994) Information coding in the olfactory system: evidence for a sterotyped and highly organized epitope map in the olfactory bulb. Cell *79*: 1245-1255.

Ring, G., R.C. Mezza, and J.E. Schwob (1997) Immunohistochemical identification of discrete subsets of rat olfactory neurons and the glomeruli that they innervate. The Journal of Comparative Neurology *388*:415-434.

Roney, K.J., A.B. Scheibel, and G.L. Shaw (1979) Dendritic bundles: survey of anatomical experiments and physiological theories. Brain Res. Rev. *1*:225-271.

Sallaz, M., and F. Jourdan (1993) C-fos expression and 2-deoxyglucose uptake in the olfactory bulb of odour-stimulated awake rats. Neuroreport *4(1)*:55-8.

Schmidt, M. and B. W. Ache (1997) Immunocytochemical analysis of glomerular regionalization and neuronal diversity in the olfactory bulb of the spiny lobster. Cell Tissue Res. *287*: 541-563.

Schmidt, M. and B.W. Ache (1992) Antennular projections to the midbrain of the spiny lobster. II. Sensory innervation of the olfactory lobe. J. Comp. Neurol. *318*: 291-303.

Scott, J.W., D.P. Wellis, M.J. Riggott, and N. Buonviso (1993) Functional organization of the main olfactory bulb. Microscopy Res. Tech. *24*: 142-156.

Shepherd, G.M. (1993) Current issues in the molecular biology of olfaction. Chemical Senses *18*:191-198.

Shepherd, G.M. and C.A. Greer (1998) Olfactory Bulb. In: The Synaptic Organization of the Brain, Shepherd G.M. (ed.), pp. 159-204, Oxford University Press, New York.

Shipley, M.T. and M. Ennis (1996) Functional organization of the olfactory system. J. Neurobiol. *30*: 123-176.

Stewart, W.B., J.S. Kauer, and G.M. Shepherd (1979) Functional organization of rat olfactory bulb analyzed by the 2-deoxyglucose method. J. Comp. Neurol. *185*: 715-734.

Stone, L.M., M.D. Browning, and T.E. Finger (1994) Differential distribution of the synapsins in the rat olfactory bulb. The Journal of Neuroscience *14*:301-309.

Südhof TC, A.J. Czernik , H-T. Kao, K. Takei, P.A. Johnson, A. Horiuchi, S.D. Kanazir, M.A. Wagner, M.S. Perin, P. De Camilli, P. Greengard (1989) Synapsins: mosaics of shared and individual domains in a family of synaptic vesicle phosphoproteins. Science *245*:1474-1480.

Thomas L, K. Hartung, D. Langosch, H. Rehm, E. Bamberg, W.W. Franke, H. Betz (1988) Identification of synaptophysin as a hexameric channel protein of the synaptic vessel membrane. Science *242*:1050-1053.

Toida, K., K. Kosaka, C. Heizmann and T. Kosaka (1998) Chemically defined neuron groups and their subpopulations in the glomerular layer of the rat main olfactory bulb: III. Structural features of calbindin D28K-immunoreactive neurons. J. Comp. Neurol. 392: 179-198.

Treloar, H., E. Walters, F. Margolis, and B. Key (1996) Olfactory glomeruli are innervated by more than one distinct subset of primary sensory olfactory neurons in mice. J. Comp. Neurol. *367*: 550-562.

Treloar, H.B., Purcell, A.L., and Greer, C.A. (1999) Glomerular formation in the developing rat olfactory bulb. The Journal of Comparative Neurology, 413: 289-304.

Treloar, H.B., V. Nurcombe, and B. Key (1996) Expression of extracellular matrix molecules in the embryonic rat olfactory pathway. Journal of Neurobiology *31(1)*:41-55.

Trombley, PQ., and GM. Shepherd (1993) Synaptic transmission and modulation in the olfactory bulb. Curr. Opin. Neurobiol. *3(4):*540-7.

Tyzio R., A. Represa, I. Jorquera, Y. Ben-Ari, H. Gozlan, L. Aniksztejn (1999) The establishment of GABAergic and glutamatergic synapses on CA1 pyramidal neurons is sequential and correlates with the development of the apical dendrite. The Journal of Neuroscience 19: 10372-10382.

Valverde, F., M. Santacana, and M. Heredia (1992) Formation of an olfactory glomerulus: morphological aspects of development and organization. Neuroscience *49*:255-275.

Vassar, R., S.K. Chao, R. Sitcheran, J.M. Nunez, L.B. Vosshall, and R. Axel (1994) Topographic organization of sensory projections to the olfactory bulb. Cell *79*:981-991.

Verhaagen J., A.B. Oestreicher, M. Grillo, Y.S. Khew-Goodall, W.H. Gispen, F.L. Margolis (1990) Neuroplasticity in the olfactory system: differential effects of central and peripheral lesions of the

Verhaagen, J., A.B. Oestreicher, W.H. Gispen, and F.L. Margolis (1989) The expression of the growth associated protein B50/GAP43 in the olfactory system of neonatal and adult rats. The Journal of Neuroscience *9*:683-691.

Vickers, N.J., T.A. Christensen, and J.G. Hildebrand (1998) Combinatorial odor discrimination in the brain: attraction and antagonist odor blends are represented in

distinct combinations of uniquely identifiable glomeruli. The Journal of Comparative Neurology *400*:35-56.

White, E.L. (1973) Synaptic organization of the mammalian olfactory glomerulus: new findings including an intraspecific variation. Brain Res. *60*: 299-313.

Zürmohle, U-M., J. Herms, R. Schlingensiepen, K-H. Schlingensiepen, W. Brysch (1994) Changes in synapsin 1 messenger RNA expression during rat brain development. Exper. Brain Res. *99*:17-24.

Figures

Page

Figure 1: An overview of the anatomy of the olfactory system....3

Figure 2: Basic synaptic circuitry of the olfactory bulb....7

Figure 3: Confocal images, reconstructed from serial optical planes, of OMP, MAP2, synaptophysin, or synapsin 1 immunoreactivity in the superficial layers of the olfactory bulb....27

Figure 4: Confocal images, reconstructed from serial optical planes, of combinations of OMP, MAP2, GFAP, synaptophysin, and synapsin 1 immunoreactivity....29

Figure 5: A glomerulus in cross section constructed from a montage of electron micrographs....35

Figure 6: High magnification electron micrographs of the rat olfactory bulb glomerulus....38

Figure 7: The frequency of axo- and dendrodendritic synapses per $40\mu m^2$ in the rat glomerulus....42

Figure 8: Light micrographs of cresyl violet stained sections of the rat olfactory bulb at postnatal days 0, 6, 12, and 18....48

Figure 9: Confocal micrographs of olfactory marker protein (OMP), growth associated protein GAP-43, and synaptophysin immunoreactivity in the superficial layers of the rat olfactory bulb at postnatal day 1....50

Figure 10: Confocal micrograph of olfactory marker protein (OMP), growth associated protein GAP-43, and synaptophysin immunoreactivity in the superficial layers of the rat olfactory bulb at postnatal day 6....52

Figure 11: Confocal micrograph of olfactory marker protein (OMP), growth associated protein GAP-43, and synaptophysin immunoreactivity in the rat olfactory bulb at postnatal day 12....54

Figure 12: Confocal micrograph of olfactory marker protein (OMP), growth associated protein GAP-43, and synaptophysin immunoreactivity in the rat olfactory bulb at postnatal day 18....56

Figure 13: Double labeled confocal images of olfactory marker protein (OMP), growth associated protein GAP-43, and synaptophysin immunoreactivity in the rat olfactory bulb at postnatal days 1, 6, 12, and 18.....60

Figure 14: Summary model of the possible organization in the mammalian glomerulus.....82

HARVEY CUSHING / JOHN HAY WHITNEY
MEDICAL LIBRARY

MANUSCRIPT THESES

Unpublished theses submitted for the Master's and Doctor's degrees and deposited in the Medical Library are to be used only with due regard to the rights of the authors. Bibliographical references may be noted, but passages must not be copied without permission of the authors, and without proper credit being given in subsequent written or published work.

This thesis by Hanna Kim has been used by the following persons, whose signatures attest their acceptance of the above restrictions.

NAME AND ADDRESS DATE